International Journal of Earth Sciences (2026) 115:26
https://doi.org/10.1007/s00531-026-02565-y

ORIGINAL PAPER

Miocene tephra horizons in the Alpine–Carpathian Foredeep and an Intra-Alpine Basin: evidence for westward dispersal of Bükkalja Volcanic Field eruptions

Lukács Réka[1,2,3] · Nehyba Slavomír[4] · Guillong Marcel[5] · Roetzel Reinhard[6] · Iglseder Christoph[6] · Harangi Szabolcs[1,3] · Ćorić Stjepan[6] · Gallhofer Daniela[7] · Petrelli Maurizio[8] · Tomanová Petrová Pavla[9]

Received: 4 November 2025 / Accepted: 15 February 2026 / Published online: 11 April 2026
© The Author(s) 2026

Abstract
Volcaniclastic layers interbedded in Miocene sedimentary successions of the Western Carpathian Foreland Basin (WCFB), North Alpine Foreland Basin (NAFB), and the Intra-Alpine Aflenz Basin represent distal fallout from large explosive eruptions. We present new zircon U–Pb ages, trace element and Hf-isotope data, and, where preserved, glass compositions to identify their sources. The results indicate derivation from successive Early to Mid-Miocene silicic eruptions of the Bükkalja Volcanic Field (BVF) in the Pannonian Basin, northern Hungary. Zircon laser ablation inductively coupled plasma–mass spectrometry ages cluster at 17 ± 0.3 Ma and 14.2 ± 0.2 Ma. Zircon Hf-isotope and trace-element compositions link the Early Miocene tephras to the 17.3 Ma Eger Ignimbrite (Hradiště) and the 16.8 Ma Bogács Ignimbrite (Ivančice-Réna, Straning). These provide the first geochemically confirmed north-western occurrence of the Eger eruption and the westernmost documented fallout from the Bogács eruption. Middle Miocene samples from the WCFB and Aflenz Basin yield slightly younger zircon ages (14.3–14.0 ± 0.2 Ma) than the 14.35 Ma Harsány Ignimbrite but display indistinguishable Hf-isotope and trace-element signatures, supporting correlation with this eruption. The new data expand the known dispersal of BVF tephras and provide firm evidence for westward ash transport. Revised zircon U–Pb ages reposition key tephra horizons within the Central Paratethys stratigraphy, shifting them to younger intervals and challenging earlier interpretations of Early Miocene marine transgressions in the WCFB and NAFB.

Keywords Zircon U–Pb geochronology · Zircon chemistry · Tephrostratigraphy · Miocene explosive volcanism · Central paratethys

Introduction

Many Central European Miocene basins, including the Alpine–Carpathian Foredeep, formed part of the epicontinental Central Paratethys Sea. However, its palaeogeographic and stratigraphic evolution remains poorly constrained (e.g., Sant et al. 2017). These semi-enclosed basins developed under varying environmental conditions and episodic connections to the Mediterranean, Indo-Pacific, and Atlantic Oceans, reflecting a complex interplay of tectonic and climatic controls (Rögl and Steininger 1983; Rögl 1998, 1999). As a result, significant uncertainties persist in correlating their sedimentary successions.

Regional stratigraphic frameworks of the Central Paratethys sub-basins are based on biozonation (planktonic foraminifera and nannofossils) combined with geodynamic and climatic events in the area, commonly expressed using sequence stratigraphic concepts (Kováč et al. 2004, 2006; Harzhauser and Piller 2007; Hohenegger et al. 2009, 2014). However, biostratigraphic and magnetostratigraphic resolutions are limited by seaway fluctuations, discontinuous sedimentation, and palaeogeographic barriers (Abdul-Azis et al. 2008; Di Stefano et al. 2011; Turco et al. 2011; Lirer et al. 2019; Gradstein et al. 2020). To overcome these challenges, the dating of tephra horizons intercalated within sedimentary successions has proven to be an effective tool for inter-basin correlation (e.g., Izett 1981; Kennett et al. 1985; Piller et al. 2007; Mandic et al. 2012, 2019; De Leeuw et al. 2013, 2018; Roetzel et al. 2014; Sant et al. 2017, 2020; Bukowski et al. 2018; Rybár et al. 2019; Šegvić et al. 2023;

Extended author information available on the last page of the article

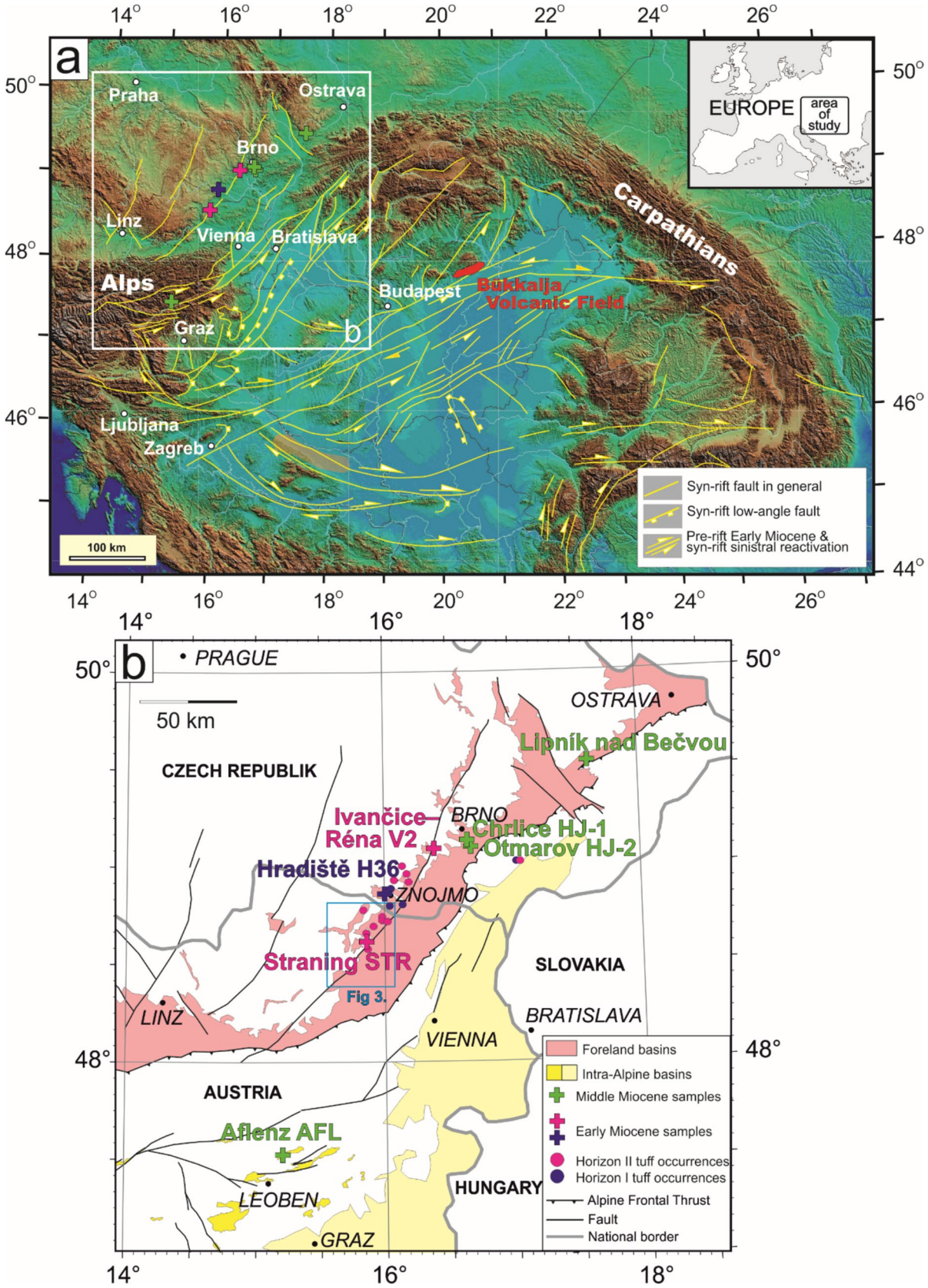
a
14°
16°
18°
20°
22°
24°
26°
50°
48°
46°
44°
Praha
Ostrava
Brno
Linz
Vienna
Bratislava
Alps
Budapest
Bükkalja
Volcanic Field
Carpathians
Graz
b
Ljubljana
Zagreb
EUROPE
area of study
100 km
Syn-rift fault in general
Syn-rift low-angle fault
Pre-rift Early Miocene & syn-rift sinistral reactivation
b
PRAGUE
50 km
OSTRAVA
Lipník nad Bečvou
CZECH REPUBLIK
Ivančice
Réna V2
BRNO
Chrlice HJ-1
Otmarov HJ-2
Hradiště H36
ZNOJMO
Straning STR
Fig 3.
SLOVAKIA
LINZ
BRATISLAVA
VIENNA
AUSTRIA
Aflenz AFL
LEOBEN
HUNGARY
GRAZ
Foreland basins
Intra-Alpine basins
Middle Miocene samples
Early Miocene samples
Horizon II tuff occurrences
Horizon I tuff occurrences
Alpine Frontal Thrust
Fault
National border

◂**Fig. 1** **a** Distribution of the investigated Early-to-Middle Miocene volcaniclastic deposits in Eastern Central Europe, showing the position of the Bükkalja Volcanic Field and the area enlarged in Fig. 1b. Abbreviations: Bp – Budapest; Bra – Bratislava; Lju – Ljubljana; **b** Study area with the regional position of the investigated samples (cross symbols) and occurrences of Horizon I and Horizon II tuffs (circle symbols), after Nehyba (1997) and Nehyba and Roetzel (1999). Symbol colours: blue – tuffs related to Horizon I; pink – tuffs related to Horizon II; green – Middle Miocene tuffs

Bercea et al. 2023; Trinajstić et al. 2023; Brlek et al. 2024a, b), especially given the extensive Miocene volcanism in the Carpathian–Pannonian region (e.g., Pécskay et al. 2006; Lukács et al. 2015, 2018, 2024; Karátson et al. 2022; Brlek et al. 2023; Harangi et al. 2025).

This study focuses on Early-to-Middle Miocene volcaniclastic deposits from the Alpine–Carpathian Foredeep, which represent the transition between the North Alpine Foreland Basin (NAFB) in the southwest and the Western Carpathian Foreland Basin (WCFB) in the northeast and the Intra-Alpine Aflenz Basin (Nehyba and Roetzel 2010; Iglseder et al. 2022). We present new age determinations and potential source correlations for these deposits, with the aim of refining the stratigraphy and correlation of the Central Paratethys sub-basins, as well as improving constraints on the spatial distribution of large silicic explosive eruptions in the Carpathian–Pannonian–Alpine region.

Geological setting

The Alpine–Carpathian Foredeep constitutes a peripheral foreland basin formed due to the tectonic emplacement and crustal loading of the Alpine–Carpathian Thrust Wedge onto the margin of the Bohemian Massif (Nehyba and Šikula 2007). The western (cratonward) margin of the Alpine–Carpathian Foredeep in the area under study (Fig. 1a-b) is formed by crystalline rocks of the Bohemian Massif and its Palaeozoic-Oligocene sedimentary cover, whilst the eastern (orogenward) margin is composed of Jurassic-to-Early Miocene deposits of the Waschberg, Ždánice, and the Subsilesian Flysch Units of the Outer Western Carpathian nappe stack (Picha et al. 2006). The stratigraphic extent of the sedimentary infill of the WCFB and the studied part of the NAFB ranges from the Oligocene/Early Miocene (Egerian) to the Middle Miocene (Upper Badenian) (Brzobohatý and Cicha 1993; Figs. 2, 3). The first Early Miocene marine flooding begun in the early Eggenburgian at the south-eastern margin of the Bohemian Massif and prograded northwestward. The onset of deposition was heterochronous due to complex palaeotopography and the influence of Neogene tectonics (Steininger and Seneš 1971; Roetzel et al. 1999). This resulted in regionally restricted and highly variable lithofacies and biofacies, giving rise to a complex lithostratigraphy in both the WCFB (in the Czech Republic; Fig. 2) and the NAFB (in Austria; Fig. 3). After a regression at the turn of the Eggenburgian and Ottnangian, the area was once again flooded by a second marine transgression in the early Ottnangian, which prograded even further northwards and westwards into small basins and former fluvial valleys on the Bohemian Massif.

Deposition in the WCFB (Fig. 2) started with the Žerotice Member (Egerian to Eggenburgian), interpreted as alluvial, fluvial, lagoonal, and distal flood plain deposits (Nehyba et al. 2019). They are overlain by Eggenburgian marine deposits (Čtyroký 1993). Dornič (1980) and Čtyroký (1982) distinguished two facies types: "marginal development" and "basin development". The marginal development is characterised by gravels and sands, fining upward into silts, sandy clays, and clays with marine and brackish mollusc and continental flora, and includes intercalations of rhyolite/rhyodacite tuff/tuffite as well as montmorillonitic and bentonitic clays in its uppermost part (Tejkal 1958; Krystek 1959; Čtyroký 1991; Knobloch 1982; Čejkovice Sand, Fig. 2). Deposits of the basin development (Dunajovice or Diváky sandstones, Dobré Pole mudstones; Adámek 2003; Fig. 2) include euhaline marine conditions with an interbed of montmorillonitic clays in their uppermost part (Batík and Čtyroký et al. 1977), correlated with tuffites in the marginal development (Čtyroký 1982) (Fig. 2). During the Ottnangian, the sea prograded towards northwest and deposited complex small-scale facies forming several lithostratigraphic units, such as the Vítonice mudstones and the Rzehakia Member (Dlabač 1976; Čtyroký 1993; Roetzel et al. 1999; Adámek 2003; Stráník et al. 2021). Around Miroslav and Ivančice, montmorillonitic clays, tuffitic clays, and/or bentonites have been reported (Čížek 1980, 1985; Kolek 1990; Čtyroký 1991). These beds can reach up to 13 m in thickness and were termed the "tuffitic member" (Dornič 1969; Dlabač 1976). However, due to the lack of more precise stratigraphic data, they are usually described as Eggenburgian–Ottnangian in age (Fig. 2).

In the studied part of the NAFB in Austria, the oldest deposits are fluvial sediments of the St. Marein-Freischling Formation in the Horn Basin (Upper Oligocene–Early Miocene) and fluvial–estuarine to lagoonal sediments of the Ravelsbach Formation on the eastern edge of the Bohemian Massif (Fig. 3) (Nehyba and Roetzel 2010; Roetzel 2017). The latter could correspond to the Žerotice Member in the WCFB. Marine flooding started in the early Eggenburgian from the south, initiating the deposition of shallow marine deposition that prograded north- and northwestwards (Roetzel et al. 1999). During the Eggenburgian and Ottnangian, two distinct marine transgressive sequences with several lithostratigraphic units developed along the south-eastern margin of the Bohemian Massif (Roetzel 1994; Roetzel et al. 1999; Mandic and Steininger 2003; Fig. 3). The first marine transgression started at the south-eastern edge of the

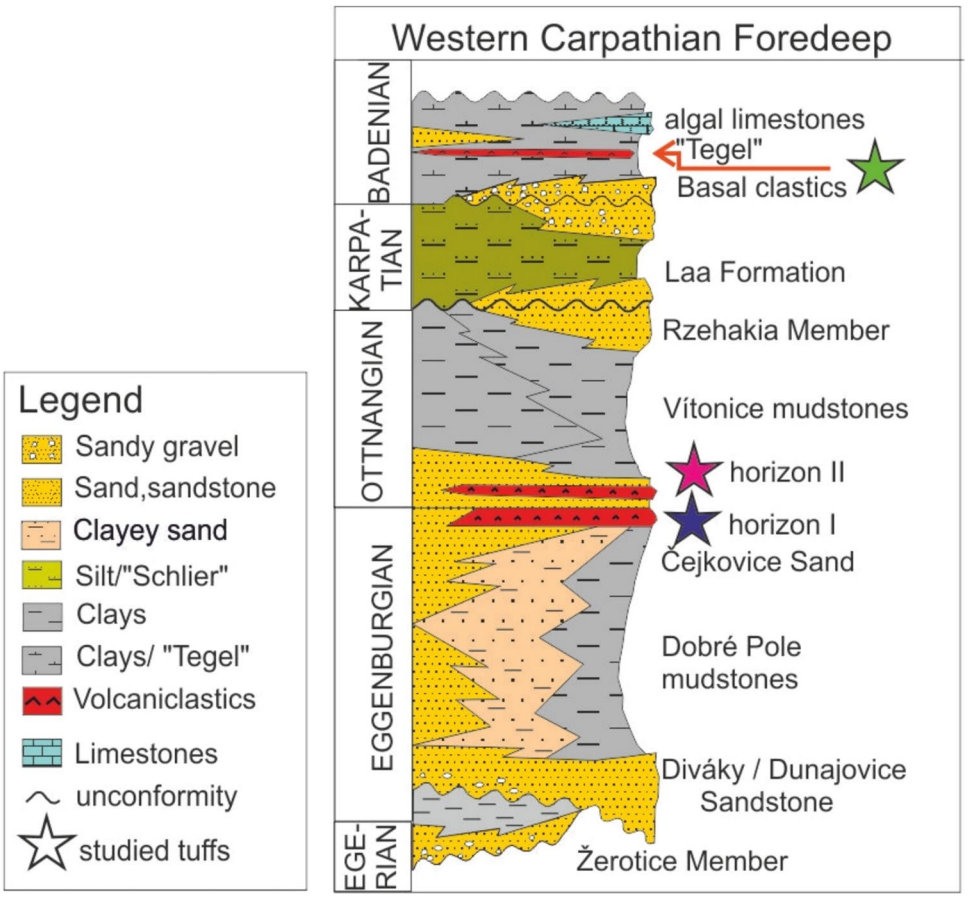

Fig. 2 Stratigraphic scheme of the sedimentary infill of the West Carpathian Foreland Basin (WCFB). Stars indicate the tuff levels occurring within the successions. The studied Hradiště H-36–4 and Ivančice Réna (V-2) samples represent the Horizon I and Horizon II tuffs, respectively. Samples HJ-2 Otmarov, HJ-1 Chrlice, and Lipník nad Bečvou (LIP) belong to the Middle Miocene tuffs within the "*Tegel*" formation

Bohemian Massif in the early Eggenburgian. It subsequently flooded the Horn Basin and reached the Eggenburg Bay in the late Eggenburgian, where the sediments were deposited directly on the crystalline basement. Sediments in the Eggenburg Bay are represented by shallow marine, wave and storm dominated sands and gravels (Burgschleinitz Fm; Pervesler et al. 1995; Nehyba and Roetzel 2022) and highly immature estuarine sediments (Kühnring Member) are laterally interfingering with it. The first transgressive cycle is completed by fine sandy to silty sediments (Gauderndorf Fm) (Roetzel et al. 1999; Mandic and Steininger 2003).

After a regression, the second transgressive cycle at the beginning of the Ottnangian starts with the Zogelsdorf Formation (Nebelsick 1989; Fig. 3). It is a fining and deepening upward succession from conglomerates, sands, sandstones, as well as coralline algae and bryozoan detritic limestones. East of the Eggenburg Bay, the Zogelsdorf Formation passes upsection into open marine clays and marls of the Zellerndorf Formation. Within the bay, the Zellerndorf Formation is restricted to deeper depressions and interfingers laterally with the Zogelsdorf Formation. Most of the Zellerndorf Formation consist of non-calcareous and smectitic silty clays. East of the Eggenburg Bay, diatomites from the Limberg Member are interfingering with the upper part of the Zellerndorf Formation (Roetzel et al. 2006; Grunert et al. 2010). From the Upper Eggenburgian until the Ottnangian, the transgression also flooded small valleys and tectonically formed basins within the Bohemian Massif, such as the basins of Langau, Riegersburg, Niederfladnitz, and Weitersfeld (Nehyba and Roetzel 1999). Smectic clays, bentonites, and tuffitic intercalations in the sediments from the Zellerndorf Formation, Weitersfeld Formation, and Langau Formation in these basins indicate volcanic input into the NAFB (Roetzel 1994; Roetzel et al. 1994; Roetzel and Řeháková 1991; Nehyba and Roetzel 1999). In marginal areas of the Langau Basin, brackish deposits from the Langau Formation occur together with lignite and tuffitic or bentonite layers (Roetzel et al. 1994).

A new marine transgression and a new depositional cycle in both the WCFB and NAFB relate to the Early Miocene stage of the Karpatian. These deposits are represented by marine calcareous silty shales from the Laa and/or Stryszawa Formations (Roetzel and Schnabel 2002; Ślączka 1977; Fig. 3). Volcaniclastics have not been reported from these deposits within the WCFB. From the NAFB, Roetzel et al. (2014) described an Early Miocene (Karpatian) silicic tuff on top of the Ottnangian Zellerndorf Formation from Straning with a $^{40}Ar/^{39}Ar$ dating of 17.23 ± 0.18 Ma. After

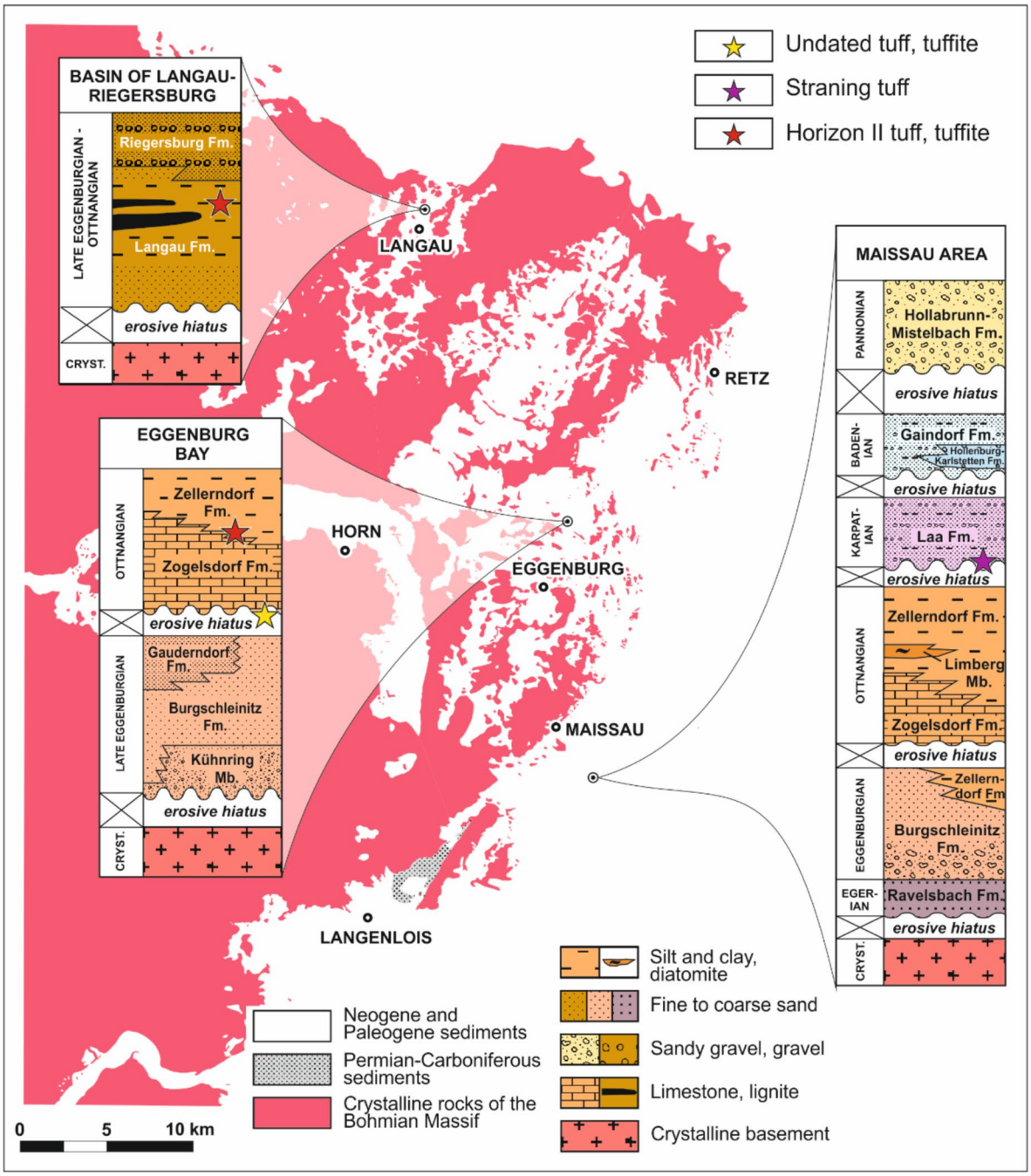

Fig. 3 Stratigraphic scheme of the sedimentary infill of the North Alpine Foreland Basin (NAFB) in the studied area. Stars indicate the tuff levels occurring within the successions. The studied Straning tuff occurs in the Maissau area. Note that all tuff occurrences are related to the Horizon II tuffs. For the undated tuff (yellow star) at the base of the Zogelsdorf Formation, see Schubert et al. (1999)

significant erosion of the older deposits and dramatic change of the Alpine–Carpathian Foredeep shape and configuration (Dellmour and Harzhauser 2012; Nehyba et al. 2022), a new deposition cycle started in the Badenian. Whilst shallow marine deposits from the Grund Formation and Gaindorf Formation are developed in the southern part of the basin, a more diverse situation was observed towards the north in the WCFB (Fig. 2). A distinctive basin infill geometry with a strong dominance of two lithofacies was recognised here (Nehyba and Šikula 2007). The first lithofacies are sandy gravels and gravelly sands (Krystek 1974; Nehyba 2018). They are commonly covered by a second dominant lithofacies, i.e., monotonous pelites ("Tegel") deposited in a marine depositional environment. The abundant fossil content provides some evidence for the NN5 Nannoplankton Zone (Tomanová Petrová and Švábenická 2007; Nehyba et al. 2008). Widespread interlayers of tuffs and tuffites have been described from the Lower Badenian succession (Nehyba 1997; Fig. 2). In the NAFB, volcaniclastics have not been described from the Lower Badenian deposits (Grund Fm, Gaindorf Fm). Middle Badenian deposition continues in the WCFB only in its northernmost part of the basin with tuffites described by Cicha et al. (1985) and Nehyba (2000).

The lateral extrusion of the Eastern Alps to the east along the Mur-Mürz Fault System (Frisch et al. 2000) during the Early and Middle Miocene led to the formation of several pull-apart basins and halfgrabens (Neubauer et al. 2000; Sachsenhofer et al. 2003). The most important pull-apart basins, which formed at the major oversteps of sinistral faults along the Mur-Mürz Fault System (Sachsenhofer et al. 2003), are Fohnsdorf Basin, Trofaiach Basin, Aflenz Basin, Leoben Basin, and Parschlug Basin. They all share a fluvial phase at the beginning of sedimentation in the Miocene, continuing with coal seams and ending with lacustrine sediments. The 16 km long and up to 2 km wide Aflenz Basin with a west-southwest–east-northeast extension was formed in the central part of the Mur-Mürz Fault System. It is bounded by Austroalpine units to the south as well to its northern margin. The basal Feistring Formation, consisting of breccias and conglomerates, represents northward and southward prograding alluvial and fluvial deposits in the Aflenz Basin. The up to 300 m-thick basal coarse-grained Feistring Formation is overlain by the Göriach Formation. The relatively small and short-lived Lake Groisenbach represents the lacustrine phase of the Aflenz Basin, where sediments from the Göriach Formation were deposited. The Göriach Formation, with a thickness of up to 200 m, is subdivided into the Groisenbach and the Sulzgraben Members. Basal coarse sediments from the Feistring Formation are overlain by three lignite seams near the base of the Göriach Formation in the eastern part of the basin (Reischenbacher and Sachsenhofer 2002). The lowest coal seam contains a rich mammal fauna, determined by Hofmann (1893) and Zapfe (1956), proving a Langhian (Badenian) age. Hajoś and Holzer (1972) investigated the occurrence of brackish diatoms from the base of the Groisenbach Member at the north-western edge of Aflenz town. The diatom associations with the genus *Stephanodiscus* are a good facies indicator, which were compared with identical occurrences in lacustrine Miocene sediments in Hungary. Based on these associations, the sediments from the Göriach Formation were assigned to the lower Badenian. Diatom associations with *Stephanodiscus* are characteristic of shallow, slightly saline freshwater palaeoconditions with quite warm temperature (Hajoś and Holzer 1972). Zorn (2015) described a Middle Miocene ostracod fauna from the Feistring Formation and the Groisenbach Member from the eastern part of the Aflenz Basin. Endemic mollusc assemblages from the Feistring Formation indicate nearshore environments with increased water energy (Harzhauser et al. 2012). The sediments from the Sulzgraben Member are developed in the western part of the Aflenz Basin (Etmißl and Sulzgraben area). They consist of grey and greenish siltstones, sandstones, and conglomerates with well-rounded components. Within this member, two tuff layers, containing a leaf flora, were discovered (Iglseder et al. 2022).

Methods

Grain-size analyses were performed using a Fritsch Laser Particle Sizer. Mean grain size, sorting, and skewness were calculated following Folk and Ward (1957). The largest clast size was estimated from the 99th percentile. Details of the analytical methods are provided in ESM_1, and reference materials with analytical results are listed in ESM_5–6.

In situ zircon U–Pb and trace-element analyses were carried out at ETH Zürich and the University of Graz using Resonetics Resolution 155 and ESI NWR 193 nm laser ablation (LA) systems coupled to Thermo Element XR and Nu Plasma II inductively coupled plasma–mass spectrometers (ICP-MS), respectively. Data reduction was performed using IOLITE (Paton et al. 2011) with the VizualAge module (Petrus and Kamber 2012). Concordant analyses were filtered based on < 10–15% discordance, and Th-disequilibrium corrections were applied as described in ESM_1. Zircon Lu–Hf isotopic analyses were performed at ETH Zürich using a Resolution 193 nm ArF laser ablation system coupled to a Nu2 MC-ICP-MS. Initial $^{176}Hf/^{177}Hf$ ratios and εHf were calculated using the crystallisation age of each sample and CHUR parameters of Bouvier et al. (2008).

Trace-element analyses of volcanic glass shards were performed at the University of Perugia (Italy) using an Agilent 8900 ICP-MS coupled to a Coherent GeoLas ArF

193 nm Excimer laser, with ATHO-G as calibration glass (Jochum et al. 2006). Concentrations were normalised to 100 wt% oxide totals (Pettke et al. 2004) using Si as the internal standard. Whole-rock major and trace elements from the Aflenz Basin were analysed by Activation Laboratories Ltd (Canada) using fusion ICP-OES/MS (procedure "4LITHO").

Micropalaeontological data are based on existing faunal lists (Brzobohatý 1982–1983) and re-evaluation of selected samples following Cicha et al. (1998). No rock samples were available for micropalaeontological study from the HJ-2 Otmarov or nearby HJ-1 Chrlice wells. Instead, we used the faunal lists compiled by R. Brzobohatý between 1982 and 1983. Clay from Lipník nad Bečvou were soaked in a Na_2CO_3 solution, and floated on 0.063 mm mesh sieve, dried, and examined under a binocular microscope. Foraminifera were identified according to Cicha et al. (1998).

Results

Samples and petrography

All samples studied in this work are shown in Fig. 1a-b and listed in Table 1 with their WGS84 coordinates. The exact stratigraphic positions of the samples are provided in ESM_2. The WCFB samples originate from the southern (boreholes Hradiště H-36, Ivančice-Réna V2, HJ-2 Otmarov, HJ-1 Chrlice) and northern (outcrop Lipník nad Bečvou) segments of the basin (Fig. 1b). Mineralogical and chemical data for these samples were presented in Novák (1978), Zádrapa (1988), Nehyba (1997), Nehyba et al. (1999), Nehyba and Roetzel (1999), Buriánek et al. (2021), and Bubík et al. (2024). Except for Lipník nad Bečvou, these samples were collected in small quantities over 30 years ago, leaving only a limited amount of material for zircon and glass separation. The study also includes a tuff sample from Straning in the NAFB, previously dated and analysed by Roetzel et al. (2014), and five samples from the Intra-Alpine

Table 1 Studied samples with their codes, locations (given as WGS84 coordinates from GPS), and the types of analyses performed. X – results obtained in this study; 0 – published results; WR – whole-rock; *paleontological data

Samples	Codes	WGS84 coordinates	Zircon U–Pb geochronology	Zircon chemistry	Zircon Lu–Hf isotopes	Glass chemistry	WR chemistry	Additional references
Western Carpathian Foreland Basin (WCFB)								
Hradiště H 36*	H36-4	N48.8608197° E16.0157842°	X	X	X	X		
Ivančice –Réna V2	IVANCICE	N49.0941675° E16.3912611°	X	X	X	0		Buriánek et al. 2021
Otmarov HJ 2*	HJ-2	N49.1019019° E16.6789978°	X	X	X	X		
Chrlice HJ-1*	HJ-1	N49.1358986° E16.6504108°				X		
Lipník nad Bečvou	LIP	N49.5341069° E17.6054033°	X	X		0		Buriánek et al. 2021
Jezernice*		N49.54244°, E17.61624°						
Aflenz Basin, Intra-Alpine Basin								
Aflenz, uppermost weathered tuff	BYG16-03/2	N47.526434° E15.205724°					X	Iglseder et al. 2022
Aflenz, upper tuff	AFL	N47.525971° E15.206221°	X	X	X	X		
Aflenz, upper tuff	BYG16-03/1	N47.526434° E15.205724°	X				X	Iglseder et al. 2022
Aflenz, upper tuff	SC10-102–16	N47.526309° E15.205797°					X	Iglseder et al. 2022
Aflenz, lower tuff	BYG18-005	N47.526334° E15.205963°	X				X	Iglseder et al. 2022
North Alpine Foreland Basin (NAFB)								
Straning	STR	N48.619167° E15.859500	X	X	X	0		Roetzel et al. 2014

Aflenz Basin, with preliminary age and chemical data published by Iglseder et al. (2022).

Sample Hradiště H36-4

The lowermost portion of the Hradiště H36 borehole (EMS_2) consists of kaolinized biotitic granite from the Thaya Batholith of Bohemian Massif. Early Miocene deposition begins with brackish-estuarine greyish-green and whitish-green sandy and silty claystones containing various mollusc assemblages, including *Pirenella moravica* (Hörn.) (Table 2), with rare occurrences even within the overlying tuffitic beds (Čtyroký et al. 1983). These deposits belong to "Eggenburgian marginal development" of Čtyroký (1993). A 20 cm-thick layer of biotite-rich whitish tuffite is interbedded within the mudstones. However, thickness of this volcaniclastic bed ranges from a few cm upto 1.5 m in the nearby area. The tuffite is horizontally laminated and graded, with biotite-enriched layers. The laminae transition from fine-grained silt at the top to medium-grained sand at the bottom. The largest clast reaches 228 µm. Sorting (σI) varies from moderately well sorted at the base to very poorly sorted at the top due to the admixture of non-volcanic particles. The light fractions include quartz, volcanic glass, and feldspar, whilst the heavy minerals are dominated by zircon, apatite, biotite, and amphibole, with rutile, staurolite, and pyroxene being less common. The glass is fresh, consisting of platy and cuspate shards, with some altered shards.

Sample Ivančice-Réna (V-2)

The lowermost portion of borehole Ivančice-Réna V-2 (EMS_2) consists of weathered granitoids from the Brno Batholith of Bohemian Massif, overlain by thick beds of reddish and green clays, with interbeds of fine-grained sand and pebble gravel. The studied 20 cm-thick whitish tuffite covers a gravel bed and is overlain by green silty clay. The tuffite is macroscopically massive, with volcanic components poorly preserved due to a significant admixture of non-volcanic material. Both platy and cuspate glass shards, pumice shards with fibrous or cellular structure, and quartz were observed. The volcanic glasses show intense alteration. Heavy minerals include apatite, zircon, amphibole, pyroxene, garnet, rutile, zoisite, and tourmaline. Above the green silty clays, an almost 1.7 m-thick bed of light grey bentonite is overlain by 90 cm of whitish silty tuffite. The Early Miocene deposition ends with more than 2 m of green and grey clays, often with interbeds of gravel and medium-grained sand. The sedimentary succession is fossil-free (Krejčí et al. 2023) and the deposits are usually described as Eggenburgian-Ottnangian in age (Dornič 1969; Dlabač 1976).

Samples HJ-2 Otmarov and HJ-1 Chrlice

In borehole HJ-2 Otmarov, two approximately 2 cm-thick whitish tuffite beds were documented at 215.2–215.6 m and 220 m. In nearby borehole HJ-1 Chrlice, about six approximately 1–4 cm-thick tuffite layers were described at depths

Table 2 Zircon U–Pb dating results of the investigated samples. Calculations were performed using $^{206}Pb/^{238}U$ dates. Abbreviations: conc. data = data with < 10% discordance; *conc. data = data with < 15% discordance; discordance is calculated as 100 × [1 – ($^{206}Pb/^{238}U$ age/$^{207}Pb/^{235}U$ age)].[a]Calculated from the dataset of each sample including the youngest dates (excluding younger outliers) towards older ones until the MSWD of the weighted average remains below a threshold value, indicating an isochronous age (Wendt and Carl 1991); [b] Propagated uncertainty was calculated by quadratic addition of the uncertainties of the weighted-mean age (including overdispersion, based on MSWD) and the external analytical uncertainty of the LA-ICP-MS measurements. The long-term excess variance of the secondary reference materials has mean values of 1.5% (ETH Zürich) and 1.3% (University of Graz), which are the main contributors to the systematic (external) error component

Locality	Sample name	No.data/conc. data*	Average uncertainity of dates	Number of data used	Youngest population age[a]	Uncertainty with 1.5% external uncertainty[b]	MSWD
			2SE		(Ma)	(Ma)	
Hradiště (H36)	H-36–4	54/43	2.65%	31	17.08	0.27	1.5
Straning	STR	52/32	3.86%	25	17.06	0.28	1.4
Ivančice –Réna (V2)	IVANCICE	46/37	2.28%	34	17.03	0.27	1.5
Lipnik n. Becvou	LIP	27/20	2.67%	9	14.12	0.25	1.7
	LIP*	27/23	2.64%	10	14.13	0.24	1.6
Aflenz	AFL	42/36	2.72%	19	14.03	0.24	1.7
	AFL*	42/38	2.72%	19	14.03	0.24	1.7
Aflenz (BYG16-03/1) upper tuff	BYG16_03	22/20	1.41%	18	14.27	0.19	0.7
Aflenz (BYG18-005) lower tuff	BYG18_005	38/32	1.88%	12	14.18	0.20	1.7
Otmarov HJ-2 (215,8-216 m)	HJ2 (220)	54/33	2.10%	19	14.34	0.23	1.3
	HJ2 (220)*	54/38	2.09%	20	14.29	0.22	1.6

between 140.5 and 158.4 m, interbedded within greyish-green clays of the "Tegel" (Fig. 2), with varying admixtures of silt and very fine sand (EMS_2). Macroscopically, the tephra layer from HJ-2 (220 m) is faintly laminated, consisting of poorly sorted very fine sand, with the coarsest clast at 195 µm. Grain-size analyses of tuffites from HJ-1 (145 m and 156 m) revealed very fine sand and coarse silt, with very poor sorting and coarsest clasts also at 195 µm. Volcanic components, including volcanic glass, quartz, and biotite, are well preserved, with only a small amount of non-pyroclastic sedimentary material. Heavy minerals include apatite, zircon, and less common amphibole, garnet, rutile, and tourmaline. The glass, dominated by platy and cuspate shards, appears fresh with partial alteration.

The sample from 215.2 to 215.4 m (HJ-2 Otmarov) is relatively poor in fossils. Benthic foraminifers, including f.e. *Ammonia beccarii* were identified (Table 2). Planktonic forams were represented by *Paragloborotalia* gr. *siakensis*, indicating the Middle Miocene age (Turco et al. 2002; Lirer et al. 2019). Siliceous spicules of sponges were also relatively abundant.

The samples from depths of 145.5–156.8 m (HJ-1 Chrlice) reveal a rich and diversified fauna, including *Uvigerina macrocarinata* with rare agglutinated foraminifera *Martinotiella communis (*Table 2*)*. Planktonic foraminifera, particularly *Globorotalia* div. sp., dominate the lower part of the succession. At 151.6 m, *Preaeorbulina glomerosa* was found and in the uppermost metre *Orbulina suturalis* along with *Praeorbulina glomerosa*. The assemblages also include gastropods and bivalves, sea-urchin spines, sponge spicules, Teleostei indet remains, and fragments of tooth of *Squalus* sp. and of the otolith *Diaphus* sp. Based on these, a deeper marine environment, an Early Badenian (Langhian) age, particularly the Lower Lagenidae zone sensu Grill (1941) and Papp et al. (1978) in the M5b *Praeorbulina glomerosa–Orbulina suturalis* zone sensu Berggren et al. (1995) was supposed, corresponding to Bukowski et al. (2018).

Sample Lipník nad Bečvou

Natural outcrops at the southwestern margin of Lipník nad Bečvou are erosional cutbanks along the downstream side of the Hlásenec stream, where several cm-thick tuffitic layers occur within monotonous green–grey mudstones. The tuff is mainly composed of altered glass (clay minerals) with few biotite flakes. The mudstones are fossil-free. Samples from a corresponding tuffite layer in a nearby clay pit near Jezernice (1 km SE) (Tišnovská et al. 1998) contain a rich microfauna (Table 2). Dominant planktonic foraminifera species like *Obandyella bykovae, Globigerinoides bisphericus,* and reworked *Globigerina ottnangiensis* were recorded. Benthic species include *Uvigerina macrocarinata, Vaginulinopsis pedum, Martinotiella karreri,* and *Pappina breviformis (*Table 2*)*. Dominant species are *Obandyella bykovae* and also *Trilobatus trilobus* and *Globigerinoides bisphericus*. The species *Globorotalia* and *Globigerinoides* suggest the Lower Badenian age, Zone M5a sensu Berggren et al. (1995), whilst *Pappina breviformis* indicates the latest Karpatian or earliest Badenian (Haunold 1990; Cicha et al. 1998) and *Globigerina ottnangiensis* is the index fossil of the Karpatian (Rögl 1994).

Sample Straning

The Straning sample comes from an outcrop within a small-scale graben in granites of the Thaya Batholith of Bohemian Massif (Fig. 3). Thin intercalations of tuff and tuffite were observed in the upper part of greenish-grey, thin, plane-bedded, non-calcareous, smectitic silty clays of the middle Burdigalian (Ottnangian) Zellerndorf Formation. The microfauna, predominantly *Silicoplacentina* sp. ("*Saccamina*") and rare *Triloculina* sp., is typical of shallow, possibly brackish-water deposits. The Straning sample was collected from the overlying tuff in the hanging wall (EMS_2). The 90 cm-thick multiphase Straning ash has a relatively constant silty grain size, with a mean between 7.53 and 2.57 µm. The tuff contains high amounts of volcanic glass, biotite, feldspar, plagioclase, quartz, ilmenite, apatite, and zircon. The silicic tuffs and tuffites were dated by $^{40}Ar/^{39}Ar$ geochronology on feldspar to 17.23 ± 0.18 Ma (Roetzel et al. 2014). These tuffs show reversed polarity and are correlated with chron C5Cr of the late Burdigalian (early Karpatian) and the lowstand systems tract (LST) of the global 3rd order sea-level cycle Bur 4 (Hardenbol et al. 1998). Further detailed data on the outcrop description, Straning granulometry, mineralogy, $^{40}Ar/^{39}Ar$ geochronology, palaeomagnetics, and geochemistry can be found in Roetzel et al. (2014).

Samples Aflenz

The Aflenz samples come from a natural outcrop in the Sulzgraben Member, along a creek in the southwestern Aflenz Basin near Sulzgraben. Within a ~ 5 m-thick sedimentary profile, two tuff layers were sampled (EMS_2). The lower part of the profile consists of 1.3 m ochre-grey and white, mica-rich clay and silt with angular local detritus (quartzite and metaignimbrite), overlain by a 20 cm-thick layer of partly rounded, altered greenish tuff components (sample BYG18-005). Above this, 90 cm of reworked tuff is capped by 1.3 m of fresh white accretionary lapilli and biotite-rich tuff (samples SC10-102–16, BYG16-03/1, AFL) containing fossil leaves. The top profile includes 30 cm of partly weathered tuff (BYG16-03/2), 30 cm grey-brown clay with plant fossils and detrital white mica, and 70 cm of well-rounded silt-sand-gravel with concretions and plant remains. The upper tuff layer contains quartz, feldspar, biotite, and

glass shards. In thin section, it exhibits a fine-grained matrix of quartz, feldspar, and biotite, with accessory apatite and zircon. Notably, accretionary lapilli up to 2.5 mm in diameter are present.

Zircon U–Pb dating

The zircon U–Pb dating results are summarised in Table 3. We analysed 27–54 spots per sample, yielding concordant data between 20 and 43 spots. Concordant data were selected with a 10% (Hradiště, Ivančice Réna) or 15% (HJ2 Otmarov, Lipník nad Bečvou) limit to increase data volume. The youngest age population was calculated for each sample, with the youngest dates selected until the MSWD of the weighted average remained below a threshold indicating isochronous age (Wendt and Carl 1991), representing the eruption age of the volcanic products (Fig. 4).

For Hradiště H36 (H-36–4), zircon dates ranged from 18.98 ± 0.65 to 16.05 ± 0.59 Ma, with the youngest population age of 17.08 ± 0.27 Ma (Fig. 4a). Ivančice Réna yielded dates from 17.86 ± 0.54 to 16.60 ± 0.34 Ma, with the youngest population age of 17.03 ± 0.27 Ma (Fig. 4b). The Straning (STR) sample showed dates between 16.54 ± 0.65 and 18.10 ± 0.56 Ma, with the youngest population age of 17.06 ± 0.28 Ma, which aligns well with the $^{40}Ar/^{39}Ar$ age of 17.23 ± 0.18 Ma (Roetzel et al. 2014) (Fig. 4 c). For HJ2 Otmarov (Fig. 4d) and Lipník nad Bečvou (Fig. 4e), Miocene dates spanned from 16.55 ± 0.81 to 13.87 ± 0.30 Ma and 15.82 ± 0.70 to 13.74 ± 0.36 Ma, respectively. Dates included 5 and 2 much older, Precambrian and Palaeozoic grain dates (638–320 Ma), respectively, and the older grains have usually weak luminescence, are rounded and slightly larger (ESM_3). Note, that the Lipník nad Bečvou sample contained only few zircon grains and the data are therefore limited. The youngest population ages were 14.29 ± 0.22 Ma (HJ2 Otmarov) and 14.13 ± 0.24 Ma (Lipník nad Bečvou).

Three tuff samples from the Aflenz Basin (Fig. 4f–h), analysed in two laboratories (ETH Zürich and University of Graz), showed overlapping $^{206}Pb/^{238}U$ dates. Two of these samples, AFL and BYG16-03/1 (Fig. 4f, h), derive from the same upper layer of the Aflenz section, whilst the third sample, BYG18-005 (Fig. 4g), originates from the lower tuff horizon. The $^{206}Pb/^{238}U$ dates of all samples overlap and show broadly similar ranges. For AFL, dates span from 17.25 ± 1.16 to 13.66 ± 0.32 Ma; for BYG16-03/1, from 14.61 ± 0.21 to 13.86 ± 0.19 Ma; and for BYG18-005 from 15.05 ± 0.35 to 14.00 ± 0.20 Ma, with two xenocrystic dates (1066.45 ± 21.34 Ma; 796.61 ± 15.97 Ma) in the latter. The youngest population ages (excluding outliers) are indistinguishable within uncertainty: 14.03 ± 0.24 Ma (AFL), 14.27 ± 0.19 Ma (BYG16-03/1), and 14.18 ± 0.20 Ma (BYG18-005).

Zircon chemistry

The Lu–Hf isotopic composition of zircon in 5 samples was measured, representing both the Ottnangian-Karpatian (H-36–4, IVANCICE, and STR) and Badenian (HJ2 and AFL) volcanic units. The εHf of studied zircons (20–53 analyses per sample) were calculated using the corresponding eruption ages. The average uncertainty (2SE) of individual εHf values is usually between 1.8 and 2.1 units. IVANCICE and STR samples yielded similar εHf values, ranging from -6.7 to -9.1 and -6.6 to -8.9, with averages -9.1 and -8.9, respectively. In contrast, sample H-36–4 shows much higher, mostly positive values, ranging from -2.4 to 5.2 with an average of 1.5 (Fig. 5). The εHf values of samples HJ2 and AFL are similar and span from -2.7 to 3.7 and -2.7 to 3.2, with averages of -0.5 and -0.2, respectively.

Trace-element composition of the dated zircon grains shows a notable variation (ESM_6). The zircon composition of the 91,500 secondary reference material (Wiedenbeck

Table 3 Identified fossil assemblages and inferred stratigraphic ages in the boreholes and outcrop localities investigated

Borehole/outcrop	Depth	Fauna	Stratigraphy
Hradiště H36-4		Molluscs: *Pirenella moravica* (Hörn.), *Cerastoderma* sp., ?*Limnopagetia* sp., *Congeria* sp., *Hydrobia* sp., *Ctyrokya* sp., *Nematurella* sp., *Melanopsis impressa* (Krauss), *Clithon* (*Vittoclithon*) *pictus* (Férussac)	Eggenburgian
Otmarov HJ-2	215.2–215.4 m	Foraminifers: *Ammonia beccarii*, *Asterigerinata planorbis*, *Nonion communis*, *Caucasina* aff. *lucera*, *Stilostomella* div. sp., *Cibicidoides* ex. gr. *ungerianus*, *Paragloborotalia* gr. *siakensis*	Middle Miocene
Chrlice HJ-1	145.5–156.8 m	*Lenticulina* div. sp., *Uvigerina* div. sp., *Melonis pompilioides*, *Pullenia bulloides*, *Hoeglundina elegans*, *Uvigerina macrocarinata*, *Martinotiella communis*, *Globorotalia* div. sp.	Lower Badenian (Langhian)
Jezernice	clay pit	*Obandyella bykovae*, *Globigerina bulloides*, *G. praebulloides*, *Trilobatus trilobus*, *Globigerinoides bisphericus*, *Globigerina ottnangiensis*, *Uvigerina macrocarinata*, *Vaginulinopsis pedum*, *Martinotiella karreri*, *Pappina breviformis*, *Globobulimina pyrula*, *Bolivina antiqua*	Lower Badenian

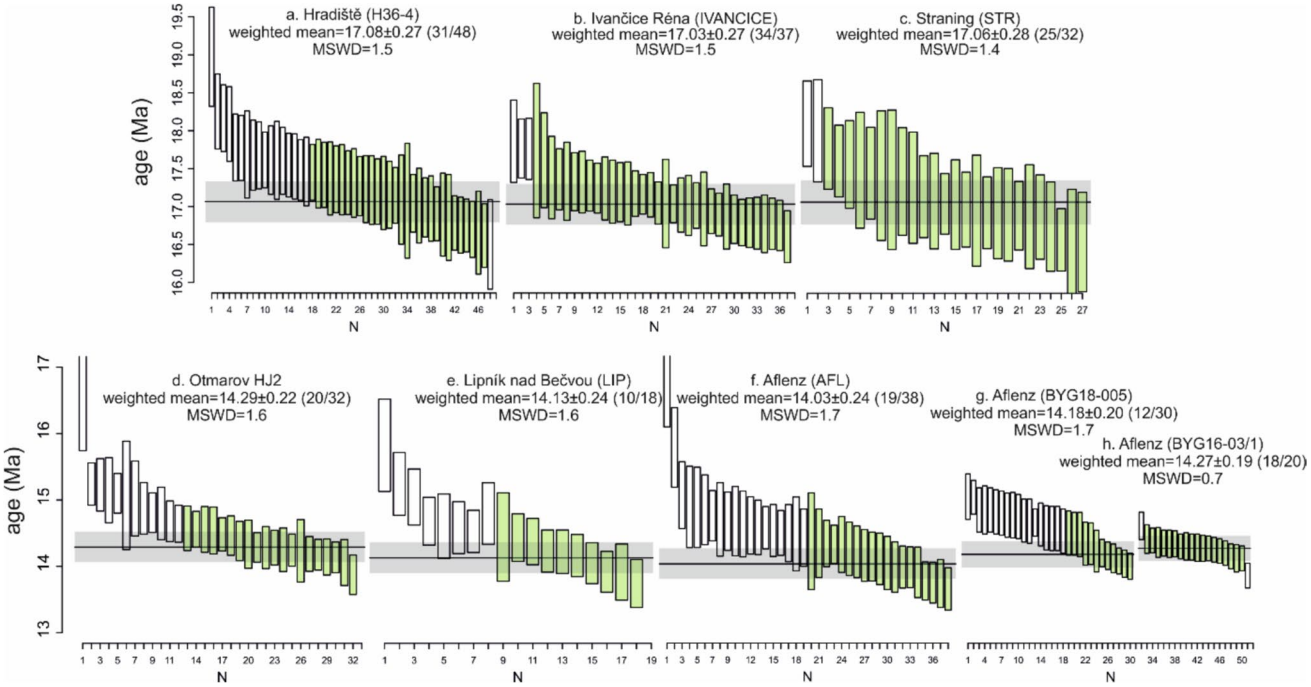

Fig. 4 **a-h** $^{206}Pb/^{238}U$ zircon dates (in Ma) of the studied samples analysed by LA-ICP-MS. Eruption ages are shown as weighted means of the youngest zircon populations (green bars) with 2σ uncertainties (grey horizontal bars). Numbers in parentheses after the ages indicate the number of dates included in the youngest population relative to the total number of concordant Miocene ages measured

et al. 1995) shows systematic differences in concentration between analytical sessions, especially for Hf; therefore, elemental ratios rather than absolute concentrations were used for interpretation (Fig. 6a-f). The observed Hf concentration offsets may result either from heterogeneity in the reference material or from uncertainty between the pulse and analogue calibration modes of the detector. Th/U ratios range between ~ 0.3 and 1.05, whilst Yb/Dy ratios span from 2.5 to 7.6 (Fig. 6a, c, e). The Eu anomaly (Eu/Eu*) ranges from 0.06 to 0.38 and the Ce-anomaly (Ce/Ce*) reaches up to 220 (calculations provided in ESM_6; Fig. 6 b, d, f). IVANCICE and STR show similar compositions and differ significantly from sample H-36–4 (Fig. 6a-d). The data of HJ2, LIP, and AFL show similar compositions, partly overlapping with IVANCICE and STR in some diagrams (Fig. 6c-f). Ti concentrations range from 1 to 17 ppm, and IVANCICE and STR show similarly variable concentrations, whereas the other samples typically reach up to ~ 6 ppm (Fig. 7). Nb concentrations overlap, ranging between 0.4 and 27 ppm for all samples except IVANCICE and STR, which display less variable values (up to 5.3 ppm) (Fig. 7). The U/Yb ratios fall between 0.4 and 3.2, typical of continental magmatic rocks (Grimes et al. 2007, 2015). Zircon Hf concentrations negatively correlate with both Th/U and with Ti contents.

Glass and bulk-rock geochemistry

We analysed the volcanic glass compositions of four apparently unaltered samples (HJ-2, HJ-1, Aflenz, and H-36–4; Fig. 8a-d). They are all rhyolitic (SiO_2 ~ 76 wt%) and have total alkali contents of 7–9 wt%, with slightly more K_2O than Na_2O ($K_2O/Na_2O = 1.2–1.5$). The HJ-1, HJ-2, and Aflenz glasses show uniform chondrite-normalised REE patterns (Fig. 8d, ESM_4) with a strong negative Eu anomaly (Eu/Eu = 0.14–0.23), whereas the H-36–4 glasses differ significantly (Fig. 8b, ESM_4), displaying more depleted medium and heavy REEs and a less-pronounced negative Eu anomaly (Eu/Eu = 0.35–0.50). The primitive mantle-normalised trace-element patterns show the same feature, i.e., remarkably uniform patterns for HJ-1, HJ-2, and Aflenz glasses, and a distinct signature for H-36–4. The latter are more enriched in Th and U and have higher Sr and slightly lower Nb contents than the glasses of the other three samples (Fig. 8a, c).

Bulk-rock geochemistry of three fresh tuff samples from the upper part of the Aflenz section yielded similar compositions (ESM_4, ESM_8), whereas the sample from the lower, slightly altered tuff differs somewhat. All samples have relatively high LOI values, with the highest (10.77–15.97 wt%) observed in the lower tuff. The normalised compositions indicate high-silica contents (75.1–77.1 and 69.3 wt%) and relatively low total alkalis (3.5–3.9 and 2.2 wt%).

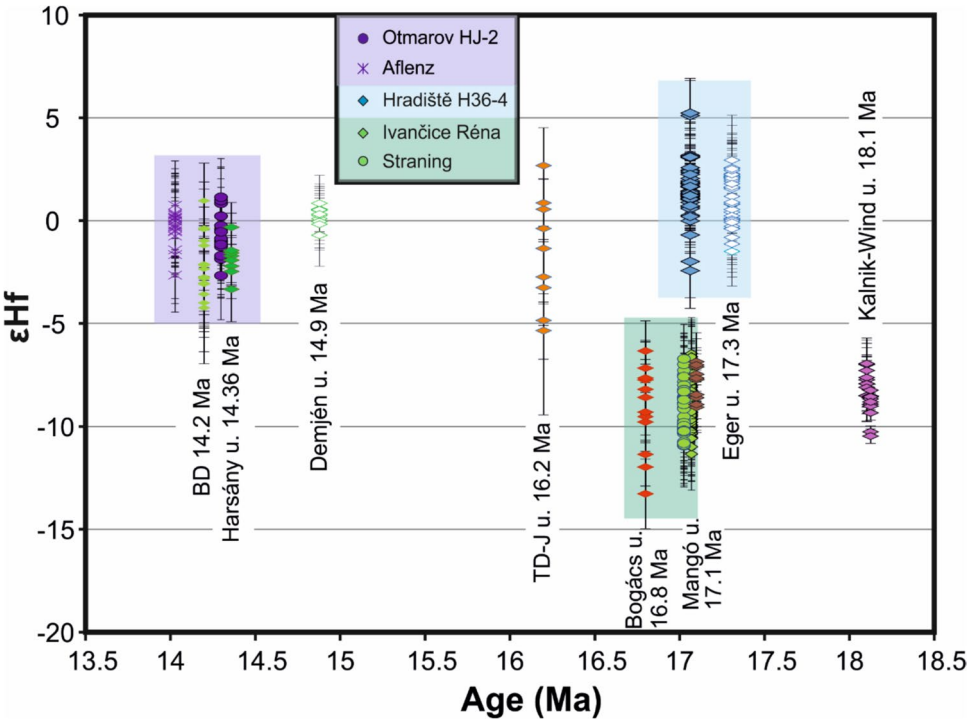

Fig. 5 Initial Hf-isotope compositions (expressed as εHf) of zircon from the studied samples (Otmarov HJ-2, Aflenz, Hradiště H-36–4, Ivančice Réna, Straning) plotted against their $^{206}Pb/^{238}U$ ages. The uncertainty of eruption ages is shown as horizontal bars coloured according to the legend. The panel also includes published εHf and eruption-age data based on CA-ID-TIMS and LA-ICP-MS $^{206}Pb/^{238}U$ analyses of Bükkalja Volcanic Field (BVF) units (Harsány u., Demjén u., Bogács u., Mangó u., Eger u., Kalnik-Wind u.; Lukács et al. 2018; Brlek et al. 2023). BD denotes a tuff deposit from the Livno–Tomislavgrad Basin (LTB), Croatia, which has distinct glass chemistry but a similar age to the Harsány unit (Brlek et al. 2024a). All eruption ages of the comparative samples have analytical uncertainties (not shown) between ~ 0.1–0.2%, except TD-J, which has 0.3% (Lukács et al. 2018; Brlek et al. 2023, 2024a,b). All εHf uncertainties are 2 SD

The three upper tuffs show consistent chondrite-normalised trace-element patterns, characterised by slightly decreasing LREE concentrations, a marked Eu anomaly ($Eu_N/Eu^* = 0.34–0.39$), and nearly flat HREEs, comparable to the glass data from Aflenz (ESM_4). The altered lower tuff shows lower concentrations of fluid-mobile elements (e.g., Ba, Rb, K, and Na), and due to alteration processes, a clear enrichment in Al and Fe is evident (ESM_8).

Discussion

Source of the Early-to-Middle Miocene tuffs

Miocene volcaniclastic layers have been reported from several sub-basins of the Central Paratethys as well as from Intra-Alpine Basins of the Eastern Alps (e.g., Ebner et al. 2002; De Leeuw et al. 2010, 2011, 2013, 2018; Mandic et al. 2012, 2019; Roetzel et al. 2014; Šegvić et al. 2014, 2023; Sant et al. 2017, 2019, 2020; Rocholl et al. 2018; Bukowski et al. 2018; Rybár et al. 2019; Badurina et al. 2021; Bercea et al. 2023; Trinajstić et al. 2023; Brlek et al. 2020, 2024b). They represent chronological snapshots of large volcanic eruptions and, therefore, play an important role to build up a temporal framework of the deposition sequences. Volcaniclastic layers of similar chronostratigraphic position and common petrographic or geochemical characteristics may be correlated across different sub-basins and used to establish regional stratigraphic key horizons. Most of the pyroclastic deposits reported in the above-cited studies are thought to derive from large, Early-to-Middle Miocene explosive eruptions in the Pannonian Basin, and are mostly associated with the volcanism of the Bükkalja Volcanic Field (BVF; Fig. 1) in north-eastern Hungary (Lukács et al. 2018). Silicic volcanism in the BVF occurred between 18.1 and 14.4 Ma (Lukács et al. 2018; Brlek et al. 2023). It comprises at least six major ignimbrite-forming eruptive units (i.e., thick and widespread; 18.1 Ma Kalnik-Wind u., 17.3 Ma Eger u., 17.1 Ma Mangó u., 16.8 Ma Bogács u., 14.9 Ma Demjén u., 14.4 Ma Harsány u.) and additional minor eruption events, each with distinct ages and/or geochemical signatures, which can form the basis for regional correlation (Harangi et al. 2005; Lukács et al. 2018, 2021, 2022; Karátson et al. 2022; Brlek et al. 2023; Hencz et al. 2024). All studied samples in this study yield ages consistent with the eruptive activity of the BVF and their grain-size parameters correspond

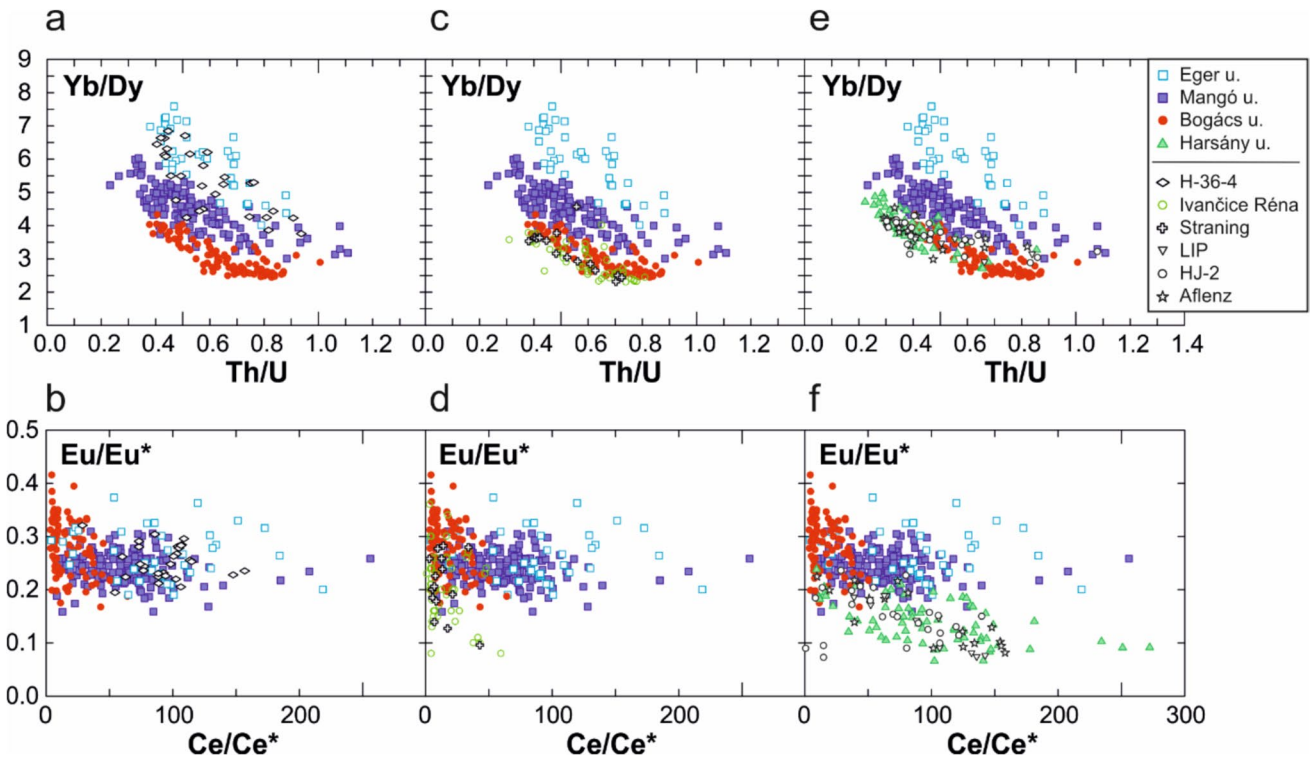

Fig. 6 **a-f** Zircon trace-element ratio plots showing compositional variations of the studied samples compared with published zircon compositions from the four closely related Early Miocene Bükkalja Volcanic Field (BVF; Lukács et al. 2021) units. a-b show data from the Hradiště H-36–4 sample, whilst **c-d** from Ivančice Réna and Straning samples in comparison with the Early Miocene 17.3 Ma Eger, 17.1 Ma Mangó, and 16.8 Ma Bogács units; **e–f** plots represent the Middle Miocene samples compared with the above units and the 14.4 Ma Harsány unit

to distal fall tephra charasteristics. Three Early Miocene samples have zircon U–Pb ages of 17.0–17.1 ± 0.3 Ma (Fig. 4), which, within uncertainty, are chronostratigraphically comparable to three main BVF units: the 17.3 Ma Eger, the 17.1 Ma Mangó, and the 16.8 Ma Bogács units. Middle Miocene samples, dated to between 14.3 and 14.0 ± 0.2 Ma, may be correlated with the youngest eruptive unit of the BVF, the extensive 14.4 Ma Harsány unit.

Lukács et al. (2021) and Brlek et al. (2023, 2024a, b) demonstrated that zircon trace-element and Hf-isotope compositions, in combination with zircon U–Pb ages and volcanic glass compositions, are reliable proxies for distinguishing between BVF units, and are thus highly effective for correlating volcaniclastic deposits over large areas. This approach is particularly valuable when correlating with altered pyroclastic deposits where the original glass composition has been modified by secondary processes. In the following, we explore correlation possibilities between the studied samples and the BVF proximal eruptive units, using zircon compositional fingerprinting and, where preservation permits, glass geochemistry (Lukács et al. 2021).

Zircon geochemistry of the Early Miocene samples indicates derivation from at least two distinct magma sources, as evidenced by contrasting zircon trace-element patterns and εHf values (Fig. 5). Sample H-36–4 from Hradiště displays more positive εHf values than the Ivančice Réna and Straning samples, suggesting a smaller contribution of crustally derived melts in the genesis of its parental magma (Fig. 5). In contrast, the remarkably similar zircon chemistry of the Ivančice Réna and Straning samples implies a shared magma source and eruptive system (Fig. 6 c-d). The elevated Yb/Dy ratios in zircons from sample H-36–4 suggest prior or coeval crystallisation of middle rare-earth element (MREE)-compatible minerals before or during zircon formation, an effect not observed in the other two samples (Fig. 6 a). Furthermore, zircon crystals from Ivančice Réna and Straning are characterised by notably higher Ti concentrations, implying higher crystallisation temperatures (Fig. 7). They also exhibit lower Ce and stronger negative Eu anomalies, potentially indicating a less-oxidised melt environment relative to the H-36–4 zircons (Fig. 6b, d). Importantly, when comparing the zircon trace-element and Hf-isotope compositions of the studied samples with those of the Early Miocene eruptive units of the BVF (Lukács et al. 2018, 2021 and Brlek et al. 2023, respectively), sample H-36–4 shows strong geochemical affinity with the 17.3 Ma Eger unit, whereas the Ivančice

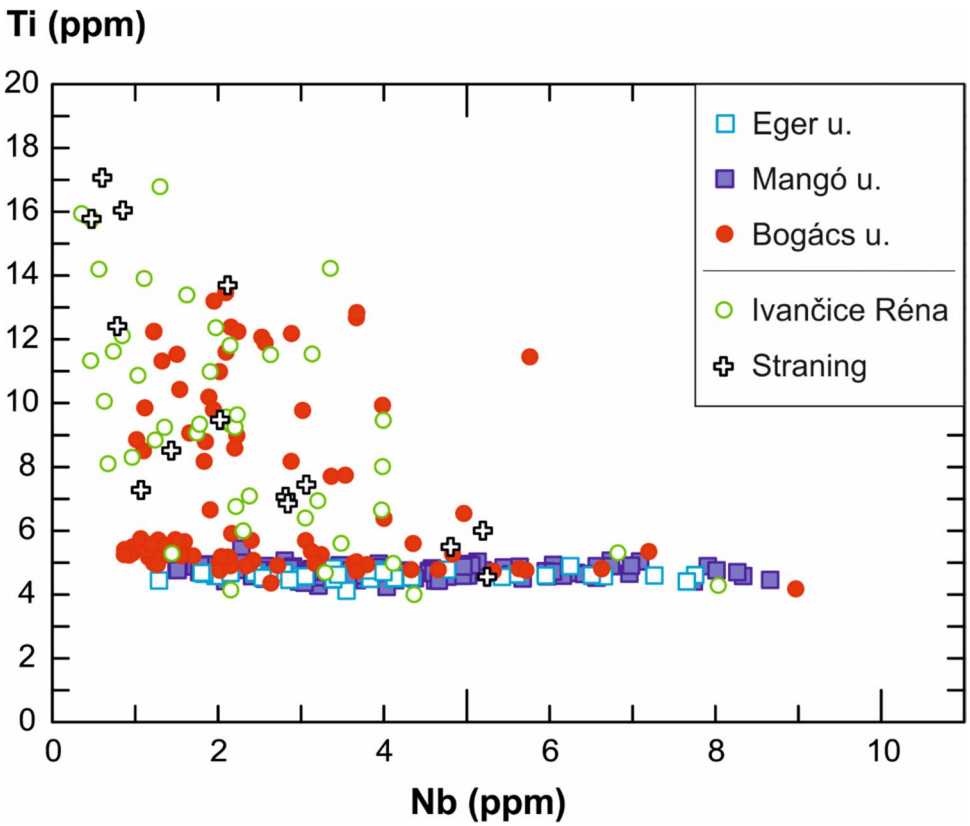

Fig. 7 Ti versus Nb concentration (ppm) in zircon, showing the distribution of the Ivančice Réna and Straning samples compared with published zircon compositions from the three closely related Early Miocene Bükkalja Volcanic Field (BVF; Lukács et al. 2021) units: 17.3 Ma Eger, 17.1 Ma Mangó, and 16.8 Ma Bogács

Réna and Straning samples are more closely aligned with the 16.8 Ma Bogács unit (Figs. 5, 6 a-d). Moreover, the observed geochemical signatures effectively exclude a correlation with the Mangó unit, despite the close similarity in eruption ages. This underscores the importance of geochemical signatures for correlation studies of volcanic deposits, particularly in cases where eruption ages are indistinguishable within the analytical uncertainty of zircon LA-ICP-MS dating.

Morphological and cathodoluminescence (CL) features of zircon crystals (ESM_3) support our interpretation on the correlation of the studied samples. Zircon typologies (sensu Pupin 1980, 1985), such as S17, S22, and S23, along with bright CL patterns, particularly in the outer crystal zones, are characteristic of the Straning (Roetzel et al. 2014) and Ivančice Réna samples and also typify zircon crystals from the Bogács unit (Szabó 2000; unpublished CL images by R. Lukács). This zircon population has relatively high typological index (I.T.) values, indicating higher crystallisation temperatures (> 750 °C). On the contrary, zircons from H-36–4 exhibit predominantly lower-indexed subtypes (S7, S8, and S9), which are consistent with crystallisation at lower temperatures (< 750 °C). The morphology of zircons in H-36–4 also closely resembles the ones observed in the Eger unit (in the lower level of the Tihamér Quarry, Eger; Szabó 2000). These morphology-based interpretations of crystallisation temperature are corroborated by Ti-in-zircon thermometry. Calculations using the thermometer of Ferry and Watson (2007) and assuming $TiO_2 = 0.6$, yield estimated crystallisation temperatures of ~ 800–850 °C for the Ivančice Réna and Straning samples, and < 750 °C for H-36–4 (cf. Lukács et al. 2021).

Fresh glass shards are available only from the sample H-36–4. They overlap with those of the 17.3 Ma Eger unit (Karátson et al. 2022; Lukács, unpublished data; Suppl. Table 4; Fig. 8 a-b, ESM_4). Although the glass in the Ivančice Réna and Straning samples is extensively argillized and thus unsuitable for in situ analysis, the published bulk-rock trace-element data for the Ivančice Réna (Buriánek et al. 2021) and Straning samples (Roetzel et al. 2014) resembles the glass compositions of the 16.8 Ma Bogács unit (Czuppon et al. 2012; Hencz et al. 2024; Fig. 8 a; ESM_4). It is important to note that the Bogács unit exhibits considerable geochemical and petrographic heterogeneity (Fig. 8 a; ESM_4), as it comprises a sequence of pyroclastic deposits originating from a chemically zoned and compositionally diverse magma reservoir (Czuppon et al. 2012). The pyroclastic succession displays a vertical transition from high-silica rhyolites containing quartz–biotite–plagioclase assemblages to more mafic dacitic and andesitic compositions, characterised by pyroxene- and plagioclase-bearing juvenile clasts. This stratigraphic progression is also reflected in the dominance of pumice clasts in the lower parts, gradually

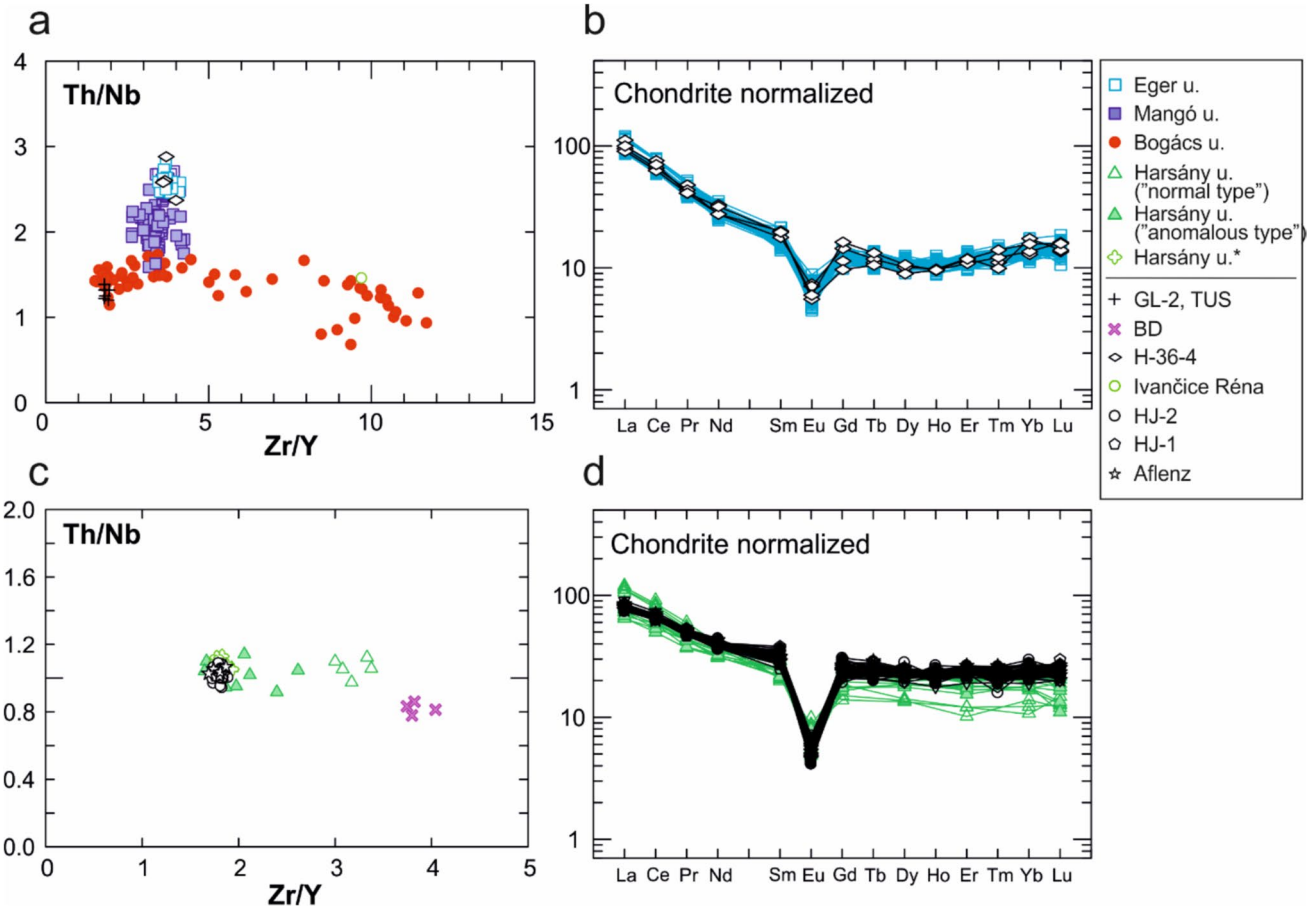

Fig. 8 Th/Nb versus Zr/Y (**a, c**) and chondrite-normalised REE multi-element (**b, d**) plots showing the trace-element compositions of glass shards from the non-altered, fresh studied samples. Plots **a-b** display data from the Hradiště H-36–4 sample (this study) and published bulk-rock values of Ivančice Réna (Buriánek et al. 2021), compared with data from the Early Miocene 17.3 Ma Eger, 17.1 Ma Mangó, and 16.8 Ma Bogács units of the Bükkalja Volcanic Field (Harangi et al. 2005; Lukács et al. 2009; Czuppon et al. 2012; Karátson et al. 2022; Hencz et al. 2024; Lukács et al. unpublished data). These are also compared with GL-2 and TUS (**a**), which represent tuff samples from the Sinj Basin (SB) and Livno–Tomislavgrad Basin (LTB), Croatia, correlated with the Bogács unit based on similar glass chemistry and bulk glass εHf signatures, and interpreted to represent the earliest eruption of the Bogács unit (Brlek et al. 2024b). Plots **c-d** show glass shard data from HJ-1, HJ-2, and Aflenz, compared with published data of the 14.4 Ma Harsány unit (Lukács et al. 2007; Hencz et al. 2024) and with 14.3 Ma BD, which denotes a tuff deposit from the Livno–Tomislavgrad Basin (LTB), Croatia, characterised by distinct glass chemistry but a similar age to the Harsány unit (Brlek et al. 2024a)

giving way to mixed and then scoria-rich layers towards the top. The trace-element composition of the Ivančice Réna and Straning bulk rocks are similar to the less-evolved hybrid-type (A-fiamme in Czuppon et al. 2012) glass of the Bogács unit. In summary, the zircon and glass trace element and zircon Hf-isotope compositions, typological results, cathodoluminescence features, and Ti-in-zircon thermometry data collectively support the correlation of sample H-36–4 with the 17.3 Ma Eger unit, and of the Ivančice Réna and Straning samples with the 16.8 Ma Bogács unit.

The younger, Middle Miocene tuff samples (HJ2, LIP, AFL, BYG18-005, and BYG16-03/1) exhibit distinct characteristics compared to the Early Miocene ones discussed above. Here, we present the results of eight variably altered tuff samples from four localities and boreholes, all of which are characterised by high-silica rhyolitic compositions. The samples yield ages of between 14.3 and 14.0 ± 0.2 Ma (Fig. 4 d-h), consistent with the LA-ICP-MS zircon age of 14.1 ± 0.3 Ma (Lukács et al. 2015) and 14.2–14.3 ± 0.2 Ma (Lukács et al. 2018) reported for the Harsány unit of the BVF. These results are slightly younger than the more precise CA-ID-TIMS and Ar–Ar ages of 14.361 ± 0.016 Ma and 14.358 ± 0.015 Ma, respectively, obtained from the same unit by Lukács et al. (2018). The discrepancy between the age interpretations was suggested to be related to matrix-dependent offsets inherent in LA-ICP-MS analyses, which were corrected following the procedures of Sliwinski et al. (2017) and applied in Lukács et al. (2018). A similar correction protocol was adopted in the present study for most samples; nevertheless, potential sources of error, such as

Pb loss, low common Pb content, or chemical mismatches between samples and primary reference materials, cannot be entirely excluded and may influence the accuracy of the LA-ICP-MS ages. Nevertheless, the LA-ICP-MS zircon ages overlap each other as well as the CA-ID-TIMS and Ar–Ar ages within uncertainties.

Bulk-rock, zircon, and glass compositions show remarkable similarity amongst all studied Middle Miocene samples (Figs. 6 e–f and 8 c-d; ESM_4). Zircon trace-element patterns from samples HJ-2, LIP, and Aflenz overlap with those of the Harsány unit, including similar ranges in Eu and Ce anomalies, Th/U, and Yb/Dy ratios. Likewise, the glass compositions of HJ-1, HJ-2, and Aflenz (and bulk-rock compositions, too) display a striking resemblance to those of the 14.4 Ma Harsány unit (Harangi et al. 2005; Lukács et al. 2021; Hencz et al. 2024), particularly to the dominant "normal type" glass found in the compositionally bimodal juvenile clast population of the unit (Lukács et al. 2009; Fig. 8 c-d, ESM_4). Epsilon Hf values from HJ-2 and Aflenz zircons also fall within the range observed in the Harsány unit (Fig. 5). These findings strongly support the interpretation that the studied tuff deposits were derived either from a single large-scale eruption, namely the Harsány ignimbrite-forming eruption event, or from temporarily closely packed multiple eruptions fed by magmas, which were geochemically indistinguishable from that of the Harsány unit. Brlek et al. (2024a) reported a chemically similar high-silica rhyolitic tuff deposit (sample BD; see ESM_4) from the Livno–Tomislavgrad Basin that yielded a slightly younger age (CA-ID-TIMS age of 14.317 ± 0.012 Ma) but displays distinct glass trace-element compositions compared to the Harsány unit. This was interpreted as evidence for more frequent explosive eruptions in the region during this time interval than previously assumed, possibly associated with the broader Harsány magmatic system.

Regional tephra correlation and ash distribution

Previous regional tephrochronological studies have identified equivalents of several eruptive units of the Bükkalja Volcanic Field (BVF), including the Kalnik–Wind, Eger, Ostoros, Mangó, Bogács, Demjén, and Harsány units, over large areas. Deposits related to four Early Miocene units (Kalnik–Wind, Eger, Mangó, and Bogács) have been reported from Croatia (Brlek et al. 2023, 2024b), where the three oldest units occur showing volcanological character of relatively proximal (pyroclastic density current) deposits in the Kalnik Mountains (North Croatia), whilst several distal fall deposits associated with the Eger, Ostoros (a minor unit stratigraphically above the Eger), and Bogács units are present in the Sinj and Livno–Tomislavgrad basins of the Dinaride Lake System. A distal tuff deposit was correlated with the Eger unit in the Eastern Carpathians Bend Zone, Romania (Bercea et al. 2023). Beyond these occurrences, another Early Miocene altered tuff horizon has been identified in the Laas area of the Intra-Alpine Fohnsdorf Basin, dated to 17.1 ± 0.7 Ma by fission-track method (Ebner et al. 2002). Additionally, Nehyba (1997) and Nehyba and Roetzel (1999) recognised two distinct widespread Early Miocene tuff horizons in the South Moravian and Lower Austrian foreland successions, based on zircon typology (Figs. 2 and 3). These were interpreted as distal fallout deposits from explosive volcanism in the Carpathian–Pannonian region (likely from North Hungary or Eastern Slovakia). In their framework, sample H-36–4 belongs to the older Horizon I, whereas Ivančice Réna represent the younger Horizon II (Figs. 2 and 3). The two horizons are typologically distinct: Horizon I contains mostly lower-indexed zircon subtypes (S4, S7, S8, S13, S14), whilst Horizon II is dominated by higher-indexed subtypes (S18, S19, S22, S23, and S24). In the wider Znojmo area, several additional localities are found and they have been assigned to Horizon I, including Strachotice, Chvalovice, Únanov, Znojmo–Pražská Street, and in boreholes Ždánice PMK-1 (87.4 m) and Ždánice-66 (745–750 m) (all in the WCFB; Figs. 1b, 2). Horizon II has been identified further north in Plaveč, Žerotice, Horní Dunajovice, Višňové, Ivančice Réna, and PMK drillings. It has also been documented in Austrian localities (in NAFB) such as Groß-Reipersdorf, Steinbruch Hattei, Retz-Süd, Unternalb–Gupferter Berg (Zellerndorf Formation), Geras B-32 (Langau Formation) and also Straning (Figs. 1b, 3). Within the BVF, the Eger and Mangó units cannot be reliably distinguished based on zircon morphology alone (Szabó 2002). Therefore, not all tuff beds containing lower-index zircon subtypes can be unequivocally assigned to the Eger unit and further zircon studies are necessary to refine the correlations. However, all the Horizon I deposits likely derived from the Early Miocene large eruptions of the BVF (Eger or Mangó).

The Bogács unit has a unique and diagnostic zircon population, making it a valuable marker for identifying its areal distribution, and extends the presence of Bogács unit in all Horizon II localities. The geochemically variable Bogács unit could represent several successive eruptions within a relatively short time fed by an early rhyolitic and a later mixed and more mafic magmas (Harangi et al. 2005; Czuppon et al. 2012; Hencz et al. 2024). This unit shows a well-distinguishable zircon trace-element signature with relatively high Ti concentrations (> 5 ppm), low Yb/Dy and high Th/U ratios, and typically low Ce/Ce* values. Zircons from the Ivančice Réna and Straning deposits share these characteristics (Figs. 6c-d and 7), which may indicate derivation from the Bogács ignimbrite-forming eruption and suggest that this event could have been a large eruption producing far-reaching ash deposits. Distal tuff correlated with the earliest Bogács unit or representing a pre-Bogács event has

been suggested in the Sinj and Livno–Tomislavgrad basins in Croatia (Brlek et al. 2024b). Samples GL-2 and TUŠ show Bogács affinity, though they represent a more silicic subgroup (ESM_4). High-precision zircon U–Pb dating of these samples extends the s.l. Bogács unit to 17.0–16.8 Ma (Brlek et al. 2024b).

Middle Miocene tuff horizons have also been widely recorded across the CPR and in adjacent regions (e.g., Sant et al. 2017; De Leeuw et al. 2013; Rocholl et al. 2018; Lukács et al. 2018, 2024). Many of these are linked to the 14.9 Ma Demjén, 14.7 Ma Tibolddaróc, and 14.4 Ma Harsány units of the BVF. A ~ 15.3 Ma rhyolitic tuff has also been documented, though its proximal source remains unknown (Rybár et al. 2019; Brlek et al. 2020). Brlek et al. (2024a) and Trinajstić et al. (2023) confirmed the existence of additional eruptions adjacent to the main BVF events, probably only distinguishable in distal records. Trinajstić et al. (2023) described the chemically distinct 14.937 ± 0.012 Ma Bidrovec eruption, related to Demjén, whilst Brlek et al. (2024a) reported a chemically slightly different 14.317 ± 0.012 Ma Harsány unit-related eruption (named as BD). Comparative layers of similar age to the studied Middle Miocene tuff samples (14.3–14.0 ± 0.2 Ma) have been reported from basins spanning from southern Germany to Bulgaria, including the NAFB, Intra-Alpine Basins, Vienna Basin, Styrian Basin, North Croatian Basin, intra-montane Dinaride basins (Sinj, Livno–Tomislavgrad, Gacko), Umbria-Marche Basin (Italy), Polish Carpathian Foredeep, Transylvanian Basin, and Maritsa East lignite basin (e.g. Ebner et al. 2002; Handler et al. 2006; De Leeuw et al. 2010, 2013, 2018; Mandic et al. 2012, 2019; Wotzlaw et al. 2014; Roetzel et al. 2014; Šegvić et al. 2023; Rocholl et al. 2018; Bukowski et al. 2018; Rybár et al. 2019; Sant et al. 2019, 2020; Arp et al. 2021; Badurina et al. 2021; Marković et al. 2021; Georgiev et al. 2022; Trinajstić et al. 2023; Brlek et al. 2024a).

The mineral assemblage of quartz, biotite, feldspar (plagioclase, sanidine), accessory zircon, apatite, Fe–Ti oxides, and allanite in high-silica rhyolite is characteristic of ~ 14.7 to 14.2 Ma pyroclastic deposits in the BVF. These are collectively referred to as Harsány-type units, including the Tibolddaróc and Harsány eruptions of the BVF. Differentiating eruptions within this interval requires high-precision dating (zircon CA-ID-TIMS or $^{40}Ar/^{39}Ar$) and, where possible, glass or zircon trace-element data (e.g., Lukács et al. 2015, 2021; Brlek et al. 2024a; Hencz et al. 2024). However, the eruption frequency and geochemical variability remain insufficiently resolved, complicating confident correlation between tuff deposits and BVF source eruptions. Despite these limitations, the broad distribution of Harsány-type tephra is evident. Based on age (14.3–14.0 ± 0.2 Ma) and chemistry, the LIP, HJ-1, HJ-2, and the Aflenz samples can be tentatively correlated with younger Harsány-type units (~ 14.4–14.25 Ma), and likely with the 14.4 Ma Harsány unit. Comparable tuffs occur in the Polish Carpathian Foredeep (14.27 ± 0.03 Ma; Bukowski et al. 2018), Transylvanian Basin (14.37 ± 0.06 Ma; De Leeuw et al. 2013), Styrian Basin (14.39 ± 0.12 Ma; Handler et al. 2006), Vienna Basin (14.31–14.03 Ma; Sant et al. 2020), Maritsa East (14.31 ± 0.30 Ma; Georgiev et al. 2022), North Alpine Foreland Basin (14.42–14.45 Ma; Rocholl et al. 2018; Dunkl et al. 2017), Umbria-Marche Basin (14.32–14.23 Ma; Wotzlaw et al. 2014), and the Ries crater (14.20 ± 0.08 Ma; Arp et al. 2021).

In summary, the new results expand the known dispersal patterns of Early-to-Middle Miocene BVF eruptions. The Straning and Ivančice–Réna occurrences together with the Horizon II localities represent the westernmost confirmed deposits of the Bogács eruption, although pre-Bogács deposits were recognised in distal settings only to the southwest, in the Sinj and Livno–Tomislavgrad basins of the Dinaride Lake System (Brlek et al. 2024b; Fig. 9). For the Eger eruption, whilst related pyroclastic flow deposits have been documented far to the southwest of the BVF in the Kalnik Mountains, distal ash-fall deposits had, until now, only been recorded from the Carpathian Bend area to the southeast (Bercea et al. 2023) and from the Sinj Basin to the south (Brlek et al. 2023; Fig. 9). The occurrence at Hradiště therefore represents the first recognised north-western outcrop of this eruption and several other Horizon I deposits might also be connected to it. Furthermore, our new results confirm the presence of tephras from the ~ 14.4 Ma Harsány eruption, or from eruptions of similar age, but the same magma type, both to the northwest (LIP, HJ-2, HJ-1) and to the west (Aflenz) of the BVF. Although the westward dispersal of these eruption(s) had been suggested in the previous studies (Lukács et al. 2018), our findings add new geochemical confirmation of this pattern (Fig. 9). Our present study shows that an integrated zircon fingerprinting is viable in the tephra correlation studies particularly in separating temporarily closely packed eruptions fed by distinct magma types (e.g., the 16.8–17.3 Ma period in the BVF). In these cases, zircon LA-ICP-MS dating alone cannot distinguish the eruptive events, whilst combined zircon geochemistry can help. On the other hand, there are cases where successive eruptions are fed by similar magma type such as during the Harsány-type eruptions in the BVF. Thus, it is important to emphasise that correlation of volcanic deposits might not be event-based, but eruptive unit-based, where the latter one comprises temporarily closely packed, i.e., within a few 100 kyr, eruptions of the same magma type.

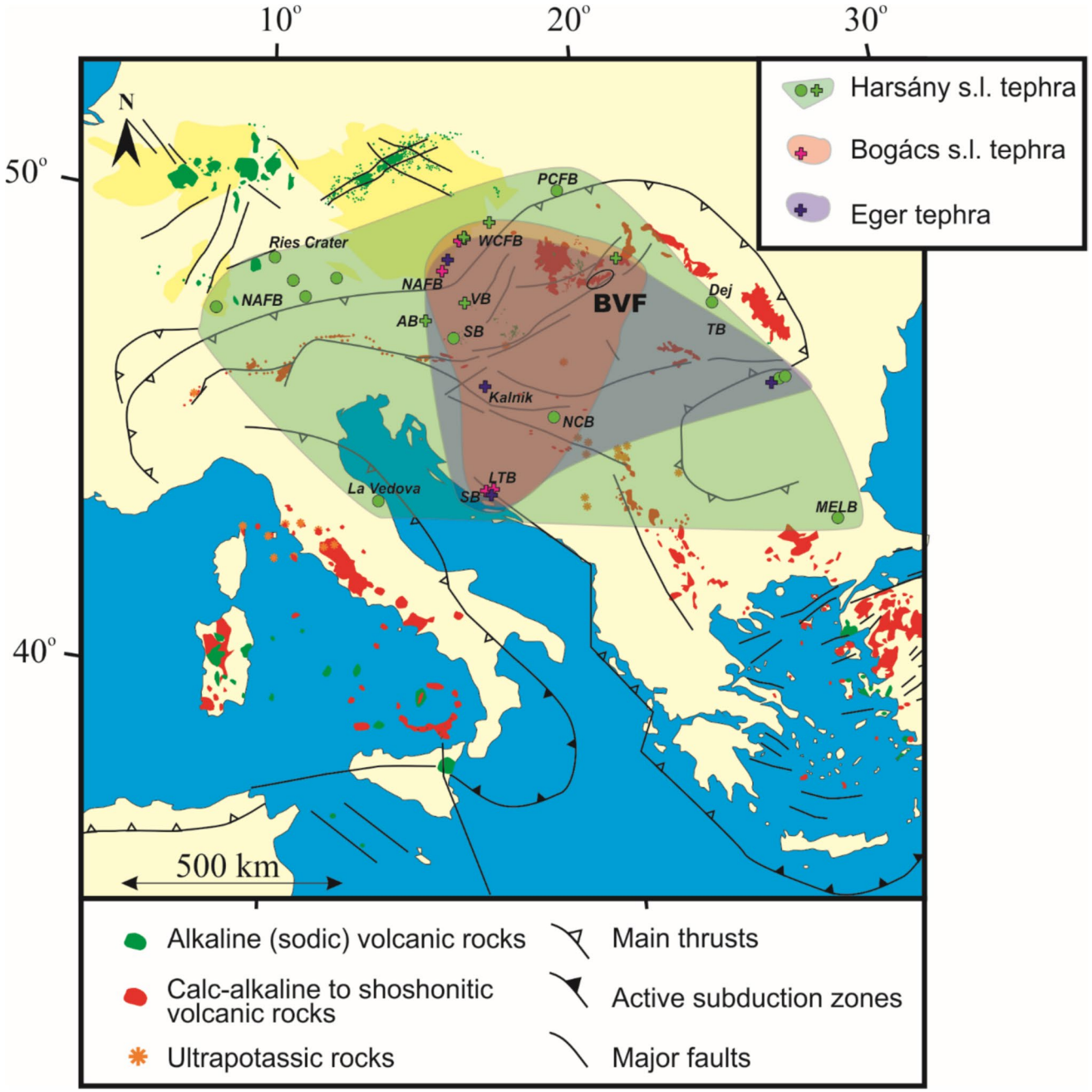

Fig. 9 Tephra dispersal of the 17.3 Ma Eger, 17.0–16.8 Ma Bogács (s.l.), and 14.7–14.2 Ma Harsány-type eruptions based on chronostratigraphic (circle symbols) and combined chrono- and chemostratigraphic (cross symbols) evidence (Ebner et al. 2002; Handler et al. 2006; De Leeuw et al. 2010, 2013, 2018; Mandic et al. 2012, 2019; Roetzel et al. 2014; Šegvić et al. 2023; Lukács et al. 2018; Rocholl et al. 2018; Bukowski et al. 2018; Rybár et al. 2019; Sant et al. 2019, 2020; Arp et al. 2021; Badurina et al. 2021; Marković et al. 2021; Georgiev et al. 2022; Brlek et al. 2020, 2024a, b; this study). Abbreviations: NAFB – North Alpine Foreland Basin; WCFB – West Carpathian Foreland Basin; PCFB – Polish Carpathian Foredeep Basin; AB – Aflenz Basin; VB – Vienna Basin; SB – Styrian Basin; NCB – North Croatian Basin; SiB – Sinj Basin; LTB – Livno–Tomislavgrad Basin; TB – Transylvanian Basin; MELB – Maritsa East Lignite Basin

Implications for the stratigraphy of the sedimentary basins

The position of the studied volcaniclastic layers within the current biostratigraphic and chronostratigraphic framework across the Early–Middle Miocene boundary (after Wade et al. 2011; Hohenegger et al. 2014; Raffi et al. 2020; Gebhardt et al. 2023) is shown in Figs. 2 and 3, which should be revised in the light of new radiometric ages. The new age data clearly indicate a late Burdigalian age (~ 17 Ma) for the older samples, corresponding to the uppermost Ottnangian to earliest Karpatian regional stages of the Central Paratethys. Consequently, the previously assumed Eggenburgian (early Burdigalian) age of these deposits must be revised. The improved precision of new radiometric data also shifts the stratigraphic position of all tuffs associated with Horizons I and II in the Czech–Austrian border area (Fig. 1b) towards younger ages (~ 17 Ma). In the light of these results, earlier stratigraphic interpretations and correlations based on these tuff layers require reassessment and adjustment. This revision also challenges previous reconstructions of the WCFB basin history, particularly the timing and extent of Eggenburgian and Ottnangian marine transgressions. A renewed, detailed lithostratigraphic evaluation and inter-basin correlation, both within the WCFB and with adjacent Central Paratethys basins, are therefore necessary. The tuffitic Horizons I and II (Nehyba 1997; Nehyba and Roetzel 1999; Nehyba et al. 1999) have traditionally served as stratigraphic markers for the boundary between the Eggenburgian (Horizon I) and Ottnangian (Horizon II) regional stages (Stráník et al. 2021). They were also used to correlate volcaniclastics in parts of the WCFB overthrust by the flysch nappes (Holzknecht and Zapletalová 1974; Zádrapa 1988), such as the volcaniclastics of the Pavlovice Formation (Eggenburgian–Karpatian; Ždánice Unit of the Western Carpathian Flysch) (Nehyba and Stráník 2005). Comparable Early Miocene tuffites from the Vienna Basin, described by Krystek (1959) and Březina (1959, 1967), may represent the same volcanic events; however, these samples are no longer available, and the published data are insufficient for a firm correlation.

The younger tuff beds deposited in the WCFB and the Aflenz Basin can be correlated with the Middle-to-Late Langhian. The Middle Langhian interval, in biostratigraphic terms, is bounded by the first occurrence of *Orbulina suturalis* (lower boundary) and the last occurrence of *Helicosphaera waltrans* (upper boundary), corresponding to a numerical age of 14.6–14.34 Ma (Holcová et al. 2024). The Late Langhian–lowermost Serravallian interval is characterised by the presence of *Sphenolithus heteromorphus* and *Orbulina spp.*, and by the absence of *Helicosphaera waltrans*, corresponding to 14.34–13.6 Ma (Holcová et al. 2024). Lower Badenian tuff horizons have been identified in numerous boreholes and outcrops throughout the WCFB (Slavík 1956; Krystek and Burkhardt 1958; Krystek 1959; Burkhardt and Molčíková 1964; Březina 1967; Říha 1984; Novák 1985; Nehyba 1997), as well as in the NAFB and sub-basins of the Pannonian Basin (e.g. Šegvić et al. 2023). Jurková and Tomšík (1959) reported 11 distinct tuff horizons in WCFB boreholes, whilst Nehyba (1997) demonstrated their uniform zircon typology, showing a dominance of typological subtypes P1 and P2 of Pupin (1980). Tuffites usually occur as several-centimetre-thick interbeds within monotonous pelites ("Tegel", Fig. 2), though locally they reach several metres. Such excessive thicknesses for distal fallout tephra suggest redeposition, further supported by the admixture of Early Miocene fossils. Offshore pelites can reach several hundred metres in thickness, and due to their monotonous nature, a simple stratigraphic subdivision is often impossible, particularly in the basin centre. Their age corresponds to the NN5 nannofossil zone and the *Orbulina suturalis–Praeorbulina glomerosa* planktonic foraminiferal Zone (Cicha et al. 1975). Dating and correlation of individual tephra horizons, combined with their spatial distribution and relationship to coeval Early Badenian lithofacies, especially the coarse-grained Gilbert-type delta deposits, have significantly improved the stratigraphic and palaeogeographic framework of the basin. These results also provide key insights into the interaction between regional and local Middle Miocene tectono-sedimentary cycles across Central Paratethys sub-basins (Haq et al. 1988; Hardenbol et al. 1998; Kováč et al. 2007, 2018; Hohenegger et al. 2014; Harzhauser et al. 2020). The Early Badenian evolution of the WCFB was characterised by northwest-directed, stepwise marine transgressions onto the basin margin, alternating with stationary or regressive phases (Nehyba et al. 2016; Holcová et al. 2018). Nehyba (2018, 2022) documented several transgressive–regressive (prograding–retrograding) cycles of marginal coarse-grained Gilbert-type deltas, reflecting repeated sea-level oscillations. Clarifying the relationship between these deltaic cycles and the transgressive–regressive trends recognised across the Central Paratethys (Kováč et al. 2006; Hohenegger et al. 2009; Abdul Aziz et al. 2008; Iaccarino et al. 2011) will help determine whether they were controlled primarily by local tectonics or basin-wide eustatic forcing. The new age data from the Aflenz Basin, together with previously published zircon fission-track ages of 14.9 ± 0.7 Ma to 15.5 ± 0.8 Ma from the Fohnsdorf and Leoben Basins (Sachsenhofer et al. 2010), provide refined chronological constraints for sedimentation in the Intra-Alpine Basins of Austria during the Middle Miocene.

Conclusions

This study refines the chronology and provenance of Early-to-Middle Miocene volcaniclastic deposits in the WCFB, the NAFB, and the Intra-Alpine Aflenz Basin. New zircon U–Pb ages, trace-element, and Hf-isotope compositions link the Early Miocene Hradiště, Ivančice–Réna, and Straning tuffs to the 17.3 Ma Eger and 16.8 Ma Bogács Ignimbrites of the Bükkalja Volcanic Field. These findings provide the first geochemically confirmed northwestern occurrences of these eruptions. Middle Miocene rhyolitic tuffs from the WCFB and Aflenz Basin yield ages of 14.3–14.0 ± 0.2 Ma and share geochemical signatures with the 14.4 Ma Harsány Ignimbrite, providing the first geochemical evidence of Harsány-type tephras northwest and west of the BVF.

The revised radiometric ages reposition several key tuff horizons within the Central Paratethys stratigraphy, challenging earlier interpretations of Early Miocene marine transgressions in the WCFB and NAFB. These findings demonstrate the power of integrating high-precision zircon geochronology, geochemistry, and morphology to trace both fresh and altered pyroclastic layers. Overall, the results refine the eruptive history and dispersal patterns of the BVF and provide an improved temporal framework for Miocene basin stratigraphy across Central Europe.

Supplementary Information The online version contains supplementary material available at https://doi.org/10.1007/s00531-026-02565-y.

Acknowledgements Univ.-Prof. Dr. Fritz Finger, University of Salzburg is acknowledged for his support in sampling and Gerhard Bryda from GeoSphere Austria for his help at sampling in the Aflenz Basin. Christian Auer is thanked for his support at the electron microscope, Andreas Wunderlich and Ibrahim Öczan for support with sample preparation. The authors thank to Mihovil Brlek and Franz Neubauer for their helpful comments and suggestions which improved the manuscript, as well as Ulrich Riller and Albrecht von Quadt for editorial work.

Author contributions Réka Lukács: conceptualization, investigation, formal analysis, visualisation, writing—original draft, and funding acquisition; Slavomír Nehyba: conceptualization, investigation, visualisation, and writing—original draft; Marcel Guillong: investigation, and writing—review & editing; Reinhard Roetzel: investigation, visualisation, and writing—original draft; Christoph Iglseder: investigation, formal analysis, visualisation, and writing—original draft; Szabolcs Harangi: investigation, visualisation, and writing—review & editing; Stjepan Ćorić: investigation, and writing—review & editing; Daniela Gallhofer: investigation, and writing—review & editing; Maurizio Petrelli: investigation, formal analysis, and writing—review & editing; Pavla Tomanová Petrová: investigation, and writing—review & editing;

Funding Open access funding provided by HUN-REN Research Centre for Astronomy and Earth Sciences. This research was supported by the National Research, Development and Innovation Office of Hungary, project OTKA K145905, and by the MTA–HUN-REN CSFK Lendület 'Momentum' PannonianVolcano Research Group (LP2024-9). Sampling was supported by the Austrian-Hungarian Action Foundation (98öu12).

Data availability All data generated or analyzed during this study are included in this article (and its supplementary information files).

Declarations

Conflict of interest The authors declare that they have no known competing financial interests or personal relationships that could have appeared to influence the work reported in this paper.

Open Access This article is licensed under a Creative Commons Attribution 4.0 International License, which permits use, sharing, adaptation, distribution and reproduction in any medium or format, as long as you give appropriate credit to the original author(s) and the source, provide a link to the Creative Commons licence, and indicate if changes were made. The images or other third party material in this article are included in the article's Creative Commons licence, unless indicated otherwise in a credit line to the material. If material is not included in the article's Creative Commons licence and your intended use is not permitted by statutory regulation or exceeds the permitted use, you will need to obtain permission directly from the copyright holder. To view a copy of this licence, visit http://creativecommons.org/licenses/by/4.0/.

References

Abdul Aziz H, Di Stefano A, Foresi LM et al (2008) Integrated stratigraphy and 40Ar/39Ar chronology of early Middle Miocene sediments from DSDP Leg 42A, Site 372 (Western Mediterranean). Palaeogeogr Palaeoclimatol Palaeoecol 257:123–138

Adámek J (2003) Miocén karpatské předhlubně na jižní Moravě, Geologický vývoj a litostratigrafické členění. Zprávy o Geologických Výzkumech v Roce 2002:9–11 ((**in Czech**))

Arp G, Dunkl I, Jung D et al (2021) A volcanic ash layer in the Nördlinger Ries impact structure (Miocene, Germany): indication of crater fill geometry and origins of long-term crater floor sagging. J Geophys Res Planets 126:e2020JE006764. https://doi.org/10.1029/2020JE006764

Badurina L, Šegvić B, Mandic O et al (2021) Miocene tuffs from the Dinarides and Eastern Alps as proxies of the Pannonian Basin lithosphere dynamics and tropospheric circulation patterns in Central Europe. J Geol Soc London 178:262. https://doi.org/10.1144/jgs2020-262

Batík P, Čtyroký P et al. (1977) Vysvětlivky k základní geologické mapě 1:25 000 list 34–131 Šatov. MS Archiv ČGÚ Praha. (in Czech)

Bercea R-I, Bălc R, Tămaş A et al (2023) Insights into the palaeoenvironments, structure and stratigraphy of the lower Miocene of the Eastern Carpathians Bend Zone, Romania. Geol Q 62(2):1–26. https://doi.org/10.7306/gq.1673

Berggren WA, Kent DV, Swisher CC III et al. (1995) A revised Cenozoic geochronology and chronostratigraphy. In: Berggren WA, Kent DV, Aubry M-P, Hardenbol J (eds) Geochronology, time scales and global stratigraphic correlation. SEPM Special Publication 54: 129–212. https://doi.org/10.2110/pec.95.04.0129

Březina J (1959) Předběžná zpráva o nových nálezech pyroklastického materiálu v miocenních sedimentech na Moravě a záp. Slovensku. Zprávy o Geologických Výzkumech v Roce 1958:14–15 ((**in Czech**))

Březina J (1967) Miocenní sedimenty karpatské předhlubně na střední Moravě – petrografická studie. Kandidátská práce, MS Geofond Praha. (in Czech)

Brlek M, Kutterolf S, Gaynor S et al (2020) Miocene syn-rift evolution of the North Croatian Basin (Carpathian–Pannonian Region): new constraints from Mts. Kalnik and Požeška gora volcaniclastic record with regional implications. Int J Earth Sci 109:2775–2800. https://doi.org/10.1007/s00531-020-01927-4

Brlek M, Tapster SR, Schindlbeck-Belo J et al (2023) Tracing widespread early Miocene ignimbrite eruptions and petrogenesis at the onset of the Carpathian-Pannonian Region silicic volcanism. Gondwana Res 116:40–60. https://doi.org/10.1016/j.gr.2022.12.015

Brlek M, Trinajstić N, Schindlbeck-Belo J et al (2024a) A distal record of the Middle Miocene silicic eruption of the Carpathian-Pannonian Region stored within the Dinaride Lake System: implications for tephrostratigraphy and emplacement of volcaniclastic deposits. Int J Earth Sci 113:1427–1455. https://doi.org/10.1007/s00531-024-02450-6

Brlek M, Trinajstić N, Gaynor SP et al (2024b) Spread and frequency of explosive silicic volcanism of the Carpathian-Pannonian Region during Early Miocene: clues from the SW Pannonian Basin and the Dinarides. J Volcanol Geotherm Res 455:108215. https://doi.org/10.1016/j.jvolgeores.2024.108215

Brzobohatý R, Cicha I (1993) Karpatská předhlubeň. In: Přichystal A, Obstová V, Suk M (eds) Geologie Moravy a Slezska. Brno. (in Czech)

Brzobohatý R, Holzknecht M (1982) Poznámka ke stratigrafii a paleogeografii eggenburgu v jižní části karpatské předhlubně na Moravě. Zemní Plyn a Nafta 27(4):353–363 ((**in Czech**))

Bubík M, Břízová E, Buriánek D et al. (2024) Basic geological map of the Czech Republic 1:25,000, 25–132 Lipník nad Bečvou with explanatory text. ČGS Praha.

Bouvier A, Vervoort JD, Patchett PJ (2008) The Lu–Hf and Sm–Nd isotopic composition of CHUR: Constraints fromunequilibrated chondrites and implications for the bulk composition of terrestrial planets. Earth and PlanetaryScience Letters 273:48–57. https://doi.org/10.1016/j.epsl.2008.06.010

Bukowski K, Sant K, Pilarz M et al (2018) Radio-isotopic age and biostratigraphic position of a lower Badenian tuffite from the western Polish Carpathian Foredeep Basin (Cieszyn area). Geol Q 62(2):303–318. https://doi.org/10.7306/gq.1402

Buriánek D, Krejčí O, Krejčí V et al. (2021) Mineralogical characteristic of secondary alteration of Miocene volcaniclastic rocks in South and Middle Moravia (Czech Republic). Geologické výzkumy na Moravě a ve Slezsku 93–104. (in Czech)

Burkhardt R, Molčíková V (1964) Nový nález tufitu z karpatské Čelní hlubiny na Moravě. Zpr Vyzk Ustavu v Olomouci 119:16–17 ((**in Czech**))

Cicha I et al (1985) Neogén v opěrných vrtech OS-1 Kravaře a OS-2 Hať v opavské pánvi. Sbor. geol. věd. Geol 40:183–229 ((**in Czech**))

Cicha I, Rögl F, Rupp C et al (1998) Oligocene-Miocene foraminifera of the Central Paratethys. Abh Senckenb Naturforsch Ges 549:1–325

Cicha I, Čtyroká J, Zapletalová I et al. (1975) East Alps and West Carpathian basins: Marine zones of benthic foraminifera. In: Cicha I (ed) Biozonal subdivision of the Upper Tertiary Basins of the Eastern Alps and West Carpathians, Proceedings of the VIth Congress RCMNS, 34–40. Geological Survey Prague.

Čížek P (1980) Výskyt bentonitu jihovýchodně od Ivančic. Geol. Průzk. 22:298–300, Praha. (in Czech)

Čížek P (1985) Výsledky výzkumu a prognózní zhodnocení surovin montmorillonitu v jihozápadní části karpatské předhlubně na Moravě. MS Archiv ČGÚ Praha. (in Czech)

Čtyroký P (1982) Spodní miocén (Eggenburg a Ottnang) jz. části Čelní hlubiny na Moravě. Zemni Plyn Nafta 27:379–394 ((**in Czech**))

Čtyroký P (1991) Členění a korelace eggenburgu a ottnangu v jižní části karpatské předhlubně na jižní Moravě. Zapadni Karpaty Ser Geol 15:67–109 ((**in Czech**))

Čtyroký P (1993) Das Tertiär der Böhmische Masse in Südmähren. Jahrb Geol Bundesanst 136:707–713

Čtyroký P, Batík P, Gabriel M et al. (1983) Vysvětlivky k základní geologické mapě ČSSR 1:25 000 list 34–113 Znojmo. ÚÚG Praha. (in Czech)

Czuppon G, Lukács R, Harangi S et al (2012) Mixing of crystal mushes and melts in the genesis of the Bogács Ignimbrite suite, northern Hungary: an integrated geochemical investigation of mineral phases and glasses. Lithos 148:71–85. https://doi.org/10.1016/j.lithos.2012.06.009

De Leeuw A, Mandic O, Vranjković A et al (2010) Chronology and integrated stratigraphy of the Miocene Sinj Basin (Dinaride Lake System, Croatia). Palaeogeogr Palaeoclimatol Palaeoecol 292:155–167. https://doi.org/10.1016/j.palaeo.2010.03.040

De Leeuw A, Mandic O, Krijgsman W et al (2011) A chronostratigraphy for the Dinaride Lake System deposits of the Livno–Tomislavgrad Basin: the rise and fall of a long-lived lacustrine environment. Stratigraphy 8:29–43

De Leeuw A, Filipescu S, Maţenco L et al (2013) Paleomagnetic and chronostratigraphic constraints on the Middle to Late Miocene evolution of the Transylvanian Basin (Romania): implications for Central Paratethys stratigraphy and emplacement of the Tisza–Dacia plate. Glob Planet Change 103:82–98. https://doi.org/10.1016/j.gloplacha.2012.04.008

De Leeuw A, Tulbure M, Kuiper KF et al (2018) New 40Ar/39Ar, magnetostratigraphic and biostratigraphic constraints on the termination of the Badenian Salinity Crisis: indications for tectonic improvement of basin interconnectivity in Southern Europe. Glob Planet Change 169:1–15. https://doi.org/10.1016/j.gloplacha.2018.07.001

Dellmour R, Harzhauser M (2012) The Iváň canyon, a large Miocene canyon in the Alpine-Carpathian Foredeep. Mar Pet Geol 38:83–94. https://doi.org/10.1016/j.marpetgeo.2012.07.001

Di Stefano A, Verducci M, Maniscalco R et al (2011) High-resolution stratigraphy of the Contrada Pesciarello borehole succession (SE Sicily): A lower Langhian reference section for the Mediterranean region. Stratigraphy 8(2):111

Dlabač M (1976) Neogén na jihovýchodním okraji Českomoravské vrchoviny. Výzk. práce ÚÚG 13u:3–22, Praha. (in Czech)

Dornič J (1969) Sedimenty staršího miocénu západně od miroslavské hrástě. Zprávy o geologických výzkumech v roce 1967 230–231, Praha. (in Czech)

Dornič J (1980) Geologické poměry neogénu jižní části karpatské předhlubně. MS Archiv ČGÚ Praha. (in Czech)

Dunkl I, Arp G, Jung D et al. (2017) Allanite as provenance indicator of volcanic ashes. Goldschmidt 2017 Conference Report, Abstract.

Ebner F, Dunkl I, Mali H et al. (2002) Stratigraphic evidence of pyroclastic layers in Miocene basins of the Eastern Alps (Austria). Geologica Carpathica 53 (Special Issue), Proceedings of XVII Congress of Carpathian–Balkan Geological Association:1–5.

Ferry JM, Watson EB (2007) New thermodynamic models and revised calibrations for the Ti-in-zircon and Zr-in-rutile thermometers. Contrib Mineral Petrol 154(4):429–437. https://doi.org/10.1007/s00410-007-0201-0

Folk RL, Ward W (1957) Brazos River bar: a study in the significance of grain-size parameters. J Sediment Res 27:3–26. https://doi.org/10.1306/74D70646-2B21-11D7-8648000102C1865D

Foresi LM, Iaccarino SM, Salvatorini G et al (2019) Mediterranean Neogene planktonic foraminifer biozonation and biochronology. Earth-Sci Rev 196:1–36. https://doi.org/10.1016/j.earscirev.2019.05.013

Frisch W, Dunkl I, Kuhlemann J (2000) Post-collisional orogen-parallel large-scale extension in the Eastern Alps. Tectonophysics 327(3–4):239–265. https://doi.org/10.1016/S0040-1951(00)00204-3

Gebhardt H, Schenk B, Enge A et al (2023) The lower–middle Miocene transition (Karpatian–Badenian) in the Krems Embayment (Central Paratethys, Lower Austria): a multistratigraphic approach and the role of the Diendorf–Boskovice Fault System. Austrian J Earth Sci 116:117–134. https://doi.org/10.17738/ajes.2023.0006

Georgiev S, Dimitrova D, Yossifova M et al (2022) Tephrochronology of a distal tonstein layer within the Maritsa East lignite basin, Bulgaria: potential sources of the Miocene large explosive eruption. Geol Carpath 73:381–387. https://doi.org/10.31577/GeolCarp.73.4.6

Gradstein FM, Ogg JG (2020) The chronostratigraphic scale. In: Gradstein FM, Ogg JD, Schmitz MD, Ogg GM (eds) Geological Time Scale 2020, vol 2, pp 21–32. https://doi.org/10.1016/B978-0-12-824360-2.00002-4

Grill R (1941) Stratigraphische Untersuchungen mit Hilfe von Mikrofaunen im Wiener Becken und den benachbarten Molasseanteilen. Oel und Kohle 37:595–602

Grimes CB, John BE, Kelemen PB et al (2007) Trace-element chemistry of zircons from oceanic crust: a method for distinguishing detrital zircon provenance. Geology 35(7):643–646. https://doi.org/10.1130/G23603A.1

Grimes CB, Wooden JL, Cheadle MJ et al (2015) Fingerprinting" tectono-magmatic provenance using trace elements in igneous zircon. Contrib Mineral Petrol 170(5):46. https://doi.org/10.1007/s00410-015-1199-3

Grunert P, Soliman A, Harzhauser M et al (2010) Upwelling conditions in the Early Miocene Central Paratethys Sea. Geol Carpathica 61:129–145

Hajoś M, Holzer H (1972) Kieselgurvorkommen im Tertiärbecken von Aflenz (Steiermark). Mitteilungen der geologischen Gesellschaft in Wien 63(1970):149–159

Handler R, Ebner F, Neubauer F et al (2006) 40Ar/39Ar dating of Miocene tuffs from the Styrian part of the Pannonian Basin: an attempt to refine the basin stratigraphy. Geol Carpathica 57:483–494

Haq BU, Hardenbol J, Vail PR (1988) Mesozoic and Cenozoic chronostratigraphy and cycles of sea-level changes. In: Wilgus CK, Hastings BS, Kendall C, Posamentier HW, Ross CA, Van Wagoner JC (eds) Sea-level changes: An integrated approach. SEPM Special Publications 42:71–108. https://doi.org/10.2110/pec.88.01.0071

Harangi S, Mason PRD, Lukács R (2005) Correlation and petrogenesis of silicic pyroclastic rocks in the Northern Pannonian Basin, Eastern-Central Europe: in situ trace element data of glass shards and mineral chemical constraints. J Volcanol Geotherm Res 143:237–257. https://doi.org/10.1016/j.jvolgeores.2004.11.012

Harangi S, Seghedi I, Lukács R (2025) The neogene–quaternary volcanism of the Carpathian–Pannonian Region: from initial plate tectonic models to quantitative petrogenetic explanations. Geol Soc Spec Publ 554:46. https://doi.org/10.1144/sp554-2024-84

Hardenbol J, Thierry J, Farley MB et al. (1998) Mesozoic and Cenozoic sequence chronostratigraphic framework of European basins. In: de Graciansky PC, Hardenbol J, Jacquin T, Vail PR (eds) Mesozoic and Cenozoic sequence stratigraphy of European basins. SEPM Special Publication 60:3–13. https://doi.org/10.2110/pec.98.02.0003

Harzhauser M, Piller WE (2007) Benchmark data of a changing sea – palaeogeography, palaeobiogeography and events in the Central Paratethys during the Miocene. Palaeogeogr Palaeoclimatol Palaeoecol 253:8–31

Harzhauser M, Neubauer TA, Mandic O et al (2012) Middle Miocene endemic freshwater mollusc assemblage from an intra-montane Alpine lake (Aflenz Basin, Eastern Alps, Austria). Palaontol Z 86:23–41. https://doi.org/10.1007/s12542-011-0117-x

Harzhauser M, Kranner M, Mandic O et al (2020) Miocene lithostratigraphy of the northern and central Vienna Basin (Austria). Aust J Earth Sci 113:169–199. https://doi.org/10.17738/ajes.2020.0011

Haunold TG (1990) The new Neogene genus *Pappina* in the new family Pappinidae; polymorphine mode of chamber addition in the Buliminacea. J Foraminiferal Res 20:56–64

Hencz M, Biró T, Németh K et al (2024) Lithostratigraphy of the ignimbrite-dominated Miocene Bükk Foreland Volcanic Area (Central Europe). J Volcanol Geotherm Res 445:107960. https://doi.org/10.1016/j.jvolgeores.2023.107960

Hofmann A (1893) Die Fauna von Göriach. Abh Geol Reichsanst 15:1–87

Hohenegger J, Rögl F, Ćorić S et al (2009) The Styrian Basin: a key to the Middle Miocene (Badenian/Langhian) Central Paratethys transgressions. Aust J Earth Sci 102:102–132

Hohenegger J, Ćorić S, Wagreich M (2014) Timing of the Middle Miocene Badenian Stage of the Central Paratethys. Geol Carpath 65:55–66. https://doi.org/10.2478/geoca-2014-0004

Holcová K, Doláková N, Nehyba S et al (2018) Timing of Langhian bioevents in the Carpathian Foredeep and northern Pannonian Basin in relation to oceanographic, tectonic and climatic processes. Geol Q 62:3–17. https://doi.org/10.7306/gq.1399

Holcová K, Scheiner F, Ackerman L et al (2024) Reliability of the Strontium Isotope Stratigraphy approach in marginal seas: insights from the Miocene Paratethys. Palaeogeogr Palaeoclimatol Palaeoecol 656:112566. https://doi.org/10.1016/j.palaeo.2024.112566

Holzknecht M, Zapletalová I (1974) Mikropaleontologické zhodnocení vrtu Dunajovice-1. MS Archiv MND Hodonín (in Czech).

Hüsing SK, Cascella A, Hilgen FJ et al (2010) Astrochronology of the Mediterranean Langhian between 15.29 and 14.17 Ma. Earth Planet Sci Lett 290:254–269. https://doi.org/10.1016/j.epsl.2009.12.002

Iaccarino SM, Di Stefano A, Foresi LM et al (2011) High-resolution integrated stratigraphy of the upper Burdigalian–lower Langhian in the Mediterranean: the Langhian historical stratotype and new candidate sections for defining its GSSP. Stratigraphy 8:199–215

Iglseder C, Bryda G, Ćorić S et al. (2022) U/Pb zircon ages on tuff in the Aflenz Basin (Styria/Austria) – Evidence for Middle Miocene widespread volcanic deposits. In: Rantitsch G, Raith JG (eds) PANGEO Austria 2022, Abstracts and Field Guides. Montanuniversität Leoben, Berichte der Geologischen Bundesanstalt 143, pp 82.

Izett GA (1981) Volcanic ash beds: recorders of Upper Cenozoic silicic pyroclastic volcanism in the western United States. J Geophys Res 86(B11):10200–10222. https://doi.org/10.1029/JB086iB11p10200

Jackson SE, Pearson NJ, Griffin WL et al (2004) The application of laser ablation–inductively coupled plasma–mass spectrometry to in situ U-Pb zircon geochronology. Chem Geol 211:47–69. https://doi.org/10.1016/j.chemgeo.2004.06.017

Jurková A, Tomšík J (1959) Tufitické horniny v tortonu ostravsko-karvínského revíru. Časopis pro Mineralogii a Geologii 4:394–407 ((**in Czech**))

Karátson D, Biró T, Portnyagin M et al (2022) Large-magnitude (VEI ≥ 7) 'wet' explosive silicic eruption preserved a Lower Miocene habitat at the Ipolytarnóc Fossil Site, North Hungary. Sci Rep 12:9743. https://doi.org/10.1038/s41598-022-13586-3

Kennett JP, von der Borch C, Baker PA et al (1985) Palaeotectonic implications of increased late Eocene–early Oligocene volcanism from South Pacific DSDP sites. Nature 316:507–511. https://doi.org/10.1038/316507a0

Knobloch E (1982) Spodnomiocénní flóry na jižní Moravě. Zemni Plyn a Nafta 27:415–428 ((**in Czech**))

Kolek P (1990) Závěrečná zpráva – Bentonity a montmorillonitové jíly. MS Archív Geologického prùzkumu Brno (in Czech).

Kováč M, Baráth I, Harzhauser M et al (2004) Miocene depositional systems and sequence stratigraphy of the Vienna Basin. Courier Forsch Inst Senckenberg 246:187–212

Kováč M, Baráth I, Fordinál K et al (2006) Late Miocene to Early Pliocene sedimentary environments and climatic changes in the Alpine–Carpathian–Pannonian junction area: a case study from the Danube Basin northern margin (Slovakia). Palaeogeogr Palaeoclimatol Palaeoecol 238:32–52. https://doi.org/10.1016/j.palaeo.2006.03.015

Kováč M, Andreyeva-Grigorovich A, Bajraktarević Z et al (2007) Badenian evolution of the Central Paratethys Sea: paleogeography, climate and eustatic sea-level changes. Geol Carpath 58:579–606

Kováč M, Halásová E, Hudáčková N et al (2018) Towards better correlation of the Central Paratethys regional time scale with the standard geological time scale of the Miocene Epoch. Geol Carpath 69:283–300

Krejčí O, Buriánek D, Krejčí V et al (2023) Lower and Middle Miocene sediments southwest of Brno in the light of new findings. Geosci Res Rep 56:59–70 ((**in Czech**))

Krystek I (1959) Petrografie tufitických hornin z oblasti vídeňské vnitrokarpatské a vněalpské pánve. Geologické Práce 54:127–144 ((**in Czech**))

Krystek I (1974) Výsledky sedimentologického výzkumu sedimentů spodního bádenu v karpatské předhlubni (na Moravě). Folia Fac Sci Nat Univ Purkynianae Brunensis, Geologia 25:1–32 ((**in Czech**))

Krystek I, Burkhardt R (1958) Lažánky (okr. Blansko) – nová lokalita tortonských tufitů na Moravě. Časopis Moravského Musea 43:75–84 ((**in Czech**))

Lukács R, Harangi S, Mason PRD et al (2009) Bimodal pumice populations in the 13.5 Ma Harsány ignimbrite, Bükkalja Volcanic Field, Northern Hungary: syn-eruptive mingling of distinct rhyolitic magma batches? Cent Eur Geol 52:51–72. https://doi.org/10.1556/CEuGeol.52.2009.1.4

Lukács R, Harangi S, Bachmann O et al (2015) Zircon geochronology and geochemistry to constrain the youngest eruption events and magma evolution of the mid-Miocene ignimbrite flare-up in the Pannonian Basin, eastern Central Europe. Contrib Mineral Petrol 170:52. https://doi.org/10.1007/s00410-015-1206-8

Lukács R, Harangi S, Guillong M et al (2018) Early to mid-Miocene syn-extensional massive silicic volcanism in the Pannonian Basin (East-Central Europe): eruption chronology, correlation potential and geodynamic implications. Earth-Sci Rev 179:1–19. https://doi.org/10.1016/j.earscirev.2018.02.005

Lukács R, Guillong M, Bachmann O et al (2021) Tephrostratigraphy and magma evolution based on combined zircon trace element and U-Pb age data: fingerprinting Miocene silicic pyroclastic rocks in the Pannonian Basin. Front Earth Sci 9:615768. https://doi.org/10.3389/feart.2021.615768

Lukács R, Harangi S, Gál P et al (2022) Formal definition and description of lithostratigraphic units related to the Miocene silicic pyroclastic rocks outcropping in Northern Hungary: a revision. Geol Carpath 73:137–158. https://doi.org/10.31577/GeolCarp.73.2.3

Lukács R, Guillong M, Szepesi J, Szymanowski D, Portnyagin M, Józsa S, Bachmann O, Petrelli M, Müller S, Schiller D, Fodor L, Chelle-Michou C, Sz Harangi (2024) Mid-Miocene silicic explosive volcanism of the Tokaj Mts., eastern-centralEurope: Eruption chronology, geochemical fingerprints and petrogenesis. Gondwaba Research 130:53–77. https://doi.org/10.1016/j.gr.2024.01.004

Mandic O, Steininger FF (2003) Computer-based mollusc stratigraphy – a case study from the Eggenburgian (Lower Miocene) type region (NE Austria). Palaeogeogr Palaeoclimatol Palaeoecol 197:263–291. https://doi.org/10.1016/S0031-0182(03)00469-3

Mandic O, de Leeuw A, Bulić J et al (2012) Paleogeographic evolution of the Southern Pannonian Basin: 40Ar/39Ar age constraints on the Miocene continental series of Northern Croatia. Int J Earth Sci 101:1033–1046. https://doi.org/10.1007/s00531-011-0695-6

Mandic O, Sant K, Kallanxhi M-E et al (2019) Integrated bio-magnetostratigraphy of the Badenian reference section Ugljevik in southern Pannonian Basin — implications for the Paratethys history (middle Miocene, Central Europe). Glob Planet Change 172:374–395. https://doi.org/10.1016/j.gloplacha.2018.10.010

Marković F, Kuiper K, Ćorić S et al (2021) Middle Miocene marine flooding: new 40Ar/39Ar age constraints with integrated biostratigraphy on tuffs from the North Croatian Basin. Geol Croat 74:237–252

Nebelsick JH (1989) Temperate water carbonate facies of the Early Miocene Paratethys (Zogelsdorf Formation, Lower Austria). Facies 21:11–39. https://doi.org/10.1007/BF02536830

Nehyba S (1997) Miocene volcaniclastics of the Carpathian Foredeep in the Czech Republic. Věstník Českého Geologického Ústavu 72:311–327

Nehyba S (2000) Vulkanoklastika středního badenu ve vrtu OS-2 Hať u Hlučína (Slezsko). Geologické Výzkumy Na Moravě a Ve Slezsku v Roce 1999 7:69–73 ((**in Czech**))

Nehyba S (2018) Lower badenian coarse-grained Gilbert deltas in the southern margin of the Western Carpathian Foredeep basin. Geol Carpath 69:89–113. https://doi.org/10.1515/geoca-2018-0006

Nehyba S, Roetzel R (1999) Lower miocene volcanoclastics in South Moravia and Lower Austria. Jb Geol B-A 141:473–490

Nehyba S, Roetzel R (2010) Fluvial deposits of the St. Marein-Freischling Formation – insights into initial depositional processes on the distal external margin of the Alpine-Carpathian Foredeep in Lower Austria. Aust J Earth Sci 103:50–80

Nehyba S, Roetzel R (2022) High-energy, microtidal nearshore deposits and their provenance (Lower Miocene, Burdigalian/Eggenburgian, Alpine-Carpathian Foredeep, Lower Austria). Geol Q 66:1–29. https://doi.org/10.7306/gq.1665

Nehyba S, Šikula J (2007) Depositional architecture, sequence stratigraphy and geodynamic development of the Carpathian Foredeep (Czech Republic). Geol Carpath 58:53–69

Nehyba S, Stráník Z (2005) Vulkanoklastika v pavlovickém souvrství ždánické jednotky. Geologické Výzkumy Na Moravě a Ve Slezsku v Roce 2004 12:37–41 ((**in Czech**))

Nehyba S, Tomanová Petrová P, Zágoršek K (2008) Sedimentological and palaeoecological records of the evolution of the southwestern part of the Carpathian Foredeep (Czech Republic) during the Early Badenian. Geol Q 52:45–60. https://doi.org/10.7306/gq.v52i1

Nehyba S, Holcová K, Gedl P et al (2016) The lower badenian transgressive–regressive cycles – a case study from Oslavany (Carpathian Foredeep, Czech Republic). Neues Jahrb Geol Palaontol Abh 279:209–238. https://doi.org/10.1127/njgpa/2016/0548

Nehyba S, Gilíková H, Tomanová Petrová P et al (2019) Evolution of a sedimentary infill of a palaeovalley at a distal margin of the peripheral foreland basin. Geol Q 63:319–344. https://doi.org/10.7306/gq.1469

Nehyba S, Roetzel R, Adamová M (1999) Tephrostratigraphy of Neogene volcaniclastics (Moravia, Lower Austria, Poland). Geol Carpath 50 (Supp), 126–127.

Neubauer F, Fritz H, Genser J et al (2000) Structural evolution within an extruding wedge: model and application to the Alpine-Pannonian system. In: Lehner FK, Urai JL (eds) Aspects of tectonic faulting (Festschrift in Honour of Georg Mandl). Springer, Berlin, pp 141–153

Novák Z (1985) Výsledky studia sedimentů miocénu (Pozdřany). Zprávy o Geologických Výzkumech v Roce 1985:139–140 ((**in Czech**))

Novák Z (1978) Petrografická charakteristika sedimentů neogénu na listu 34–113 Znojmo. MS Geofond Praha. (in Czech)

Papp A, Cicha I, Seneš J (1978) Gliederung des Badenien, Faunenzone und Unterstufen. In: Papp A, Cicha I, Seneš J, Steininger F (eds) M4 badenien (Moravien, Wielicien, Kosovien). Chronostratigraphie und Neostratotypen, Miozän der zentralen Paratethys 6. VEDA, Bratislava, pp 49–52

Paton C, Hellstrom J, Paul B et al (2011) Iolite: freeware for the visualisation and processing of mass spectrometric data. J Anal at Spectrom 26:2508–2518. https://doi.org/10.1039/c1ja10172b

Pécskay Z, Lexa J, Szakács A et al (2006) Geochronology of Neogene magmatism in the Carpathian arc and intra-Carpathian area. Geol Carpath 57:511–530

Pervesler P, Roetzel R, Steininger FF (1995) Taphonomie der Sirenen in den marinen Flachwasserablagerungen (Burgschleinitz-Formation, Eggenburgium, Untermiozän) der Gemeindesandgrube Kühnring (Niederösterreich). Jb Geol B-A 138:89–121

Petrus JA, Kamber BS (2012) VizualAge: a novel approach to laser ablation ICP-MS U-Pb geochronology data reduction. Geostand Geoanal Res 36:247–270. https://doi.org/10.1111/j.1751-908X.2012.00158.x

Pettke T, Halter WE, Webster JD et al. (2004) Accurate quantification of melt inclusion chemistry by LA-ICPMS: a comparison with EMP and SIMS and advantages and possible limitations of these methods. Lithos 78:333–351. https://doi.org/10.1016/j.lithos.2004.06.011

Picha FJ, Stránik Z, Krejčí O (2006) Geology and hydrocarbon resources of the outer Western Carpathians and their foreland, Czech Republic. In: Golonka J, Picha FJ (eds) The Carpathians and their foreland: Geology and hydrocarbon resources. AAPG Memoir 84, pp 49–175. https://doi.org/10.1306/985607M843067

Piller WE, Harzhauser M, Mandic O (2007) Miocene Central Paratethys stratigraphy – current status and future directions. Stratigraphy 4:151–168. https://doi.org/10.29041/strat.04.2.09

Pupin JP (1980) Zircon and granite petrology. Contrib Mineral Petrol 73:207–220

Pupin JP (1985) Magmatic zoning of Hercynian granitoids in France based on zircon typology. Schweiz Mineral Petrogr Mitt 65:29–56

Raffi I, Wade BS, Pälike H et al. (2020) The Neogene Period. In: Gradstein FM, Ogg JD, Schmitz MD, Ogg GM (eds) Geological Time Scale 2020 2:1141–1215. https://doi.org/10.1016/B978-0-12-824360-2.00029-2

Reischenbacher D, Sachsenhofer RF (2002) Das Miozän des Aflenzer Beckens. PanGeo Austria: Erdwissenschaften in Österreich 28.–30.6.2002, Salzburg: Programm und Kurzfassungen 144–145.

Říha J (1984) Mikrofauistická společenstva vrteb Ostopovice HV-210 a Žebětín HV-211 u Brna. Acta Musei Moraviae Sci Nat 69:207–208 ((**in Czech**))

Rocholl A, Schaltegger U, Gilg HA et al (2018) The age of volcanic tuffs from the Upper Freshwater Molasse (North Alpine Foreland Basin) and their possible use for tephrostratigraphic correlations across Europe for the Middle Miocene. Int J Earth Sci 107:387–407. https://doi.org/10.1007/s00531-017-1499-0

Roetzel R (1994) Bericht 1993 über geologische Aufnahmen im Tertiär und Quartär im Raum Grafenberg-Maissau auf Blatt 22 Hollabrunn. Jb Geol B-A 137:435–438

Roetzel R (2017) Bericht 2013–2016 über geologische Aufnahmen auf Blatt 21 Horn. Jb Geol B-A 157:317–328

Roetzel R, Schnabel W (2002) Molasse, Waschbergzone, Paläogen und Neogen auf der Böhmischen Masse. Legende und kurze Erläuterungen zur geologischen Karte von Niederösterreich 1:200.000. Geologische Bundesanstalt, Wien, pp 23–30

Roetzel R, Ćorić S, Galović I et al (2006) Early Miocene (Ottnangian) coastal upwelling conditions along the southeastern scarp of the Bohemian Massif (Parisdorf, Lower Austria, Central Paratethys). Beitr Paläontol 30:387–413

Roetzel R, de Leeuw A, Mandic O et al (2014) Lower Miocene (upper Burdigalian, Karpatian) volcanic ash-fall at the south-eastern margin of the Bohemian Massif in Austria – New evidence from 40Ar/39Ar-dating, palaeomagnetic, geochemical and mineralogical investigations. Aust J Earth Sci 107:2–22

Roetzel R, Řeháková Z (1991) Haltepunkt 20 Weitersfeld Lagerhaus. In: Roetzel R (ed) Geologie am Ostrand der Böhmische Masse in Niederösterreich. Schwerpunkt Blatt 21 Horn, Arbeitstagung der Geologischen Bundesanstalt, Eggenburg 16.–20.9.1991, pp 204–206.

Roetzel R, Ottner F, Schwaighofer B et al. (1994) Tertiäre Tone am Ostrand der Böhmischen Masse. In: Kohler EE (ed) Berichte der dt. Ton- und Tonmineralgruppe e.V. Beiträge zur Jahrestagung Regensburg, 13.–14. Okt. 1994, Regensburg, pp 111–122.

Roetzel R, Mandic O, Steininger FF (1999) Lithostratigraphie und Chronostratigraphie der tertiären Sedimente im westlichen Weinviertel und angrenzenden Waldviertel. In: Roetzel R (ed) Arbeitstagung der Geologischen Bundesanstalt 1999, Retz–Hollabrunn, 3.–7. Mai 1999, pp 38–54.

Rögl F (1994) *Globigerina ciperoensis* (Foraminiferida) in the Oligocene and Miocene of the Central Paratethys. Ann Naturhist Mus Wien 94A:133–159

Rögl F (1998) Palaeogeographic considerations for Mediterranean and Paratethys seaways (Oligocene to Miocene). Ann Naturhist Mus Wien 99A:279–310

Rögl F (1999) Mediterranean and Paratethys. Facts and hypotheses of an Oligocene to Miocene paleogeography (short overview). Geol Carpath 50:339–349

Rögl F, Steininger FF (1983) Vom Zerfall der Tethys zu Mediterran und Paratethys. Die neogene Paläogeographie und Palinspastik des zirkum-mediterranen Raumes. Ann Naturhist Mus Wien 85A:135–163

Rybár S, Šarinová K, Sant K et al (2019) New 40Ar/39Ar, fission track and sedimentological data on a middle Miocene tuff occurring in the Vienna Basin: implications for the northwestern Central Paratethys region. Geol Carpath 70:386–404. https://doi.org/10.2478/geoca-2019-0022

Sachsenhofer RF, Bechtel A, Reischenbacher D et al (2003) Evolution of lacustrine systems along the Miocene Mur-Mürz fault system (Eastern Alps, Austria) and implications on source rocks in pull-apart basins. Mar Pet Geol 20:83–110. https://doi.org/10.1016/S0264-8172(03)00018-7

Sachsenhofer RF, Gruber W, Dunkl I (2010) Das Miozän der Becken von Leoben und Fohnsdorf. J Alpine Geol 53:9–38 ((**in German**))

Sant K, Palcu DV, Mandic O et al (2017) Changing seas in the Early-Middle Miocene of Central Europe: a Mediterranean approach to Paratethyan stratigraphy. Terra Nova 29:273–281. https://doi.org/10.1111/ter.12273

Sant K, Palcu D, Turco E et al (2019) The mid-Langhian flooding in the eastern Central Paratethys: integrated stratigraphic data from the Transylvanian Basin and SE Carpathian Foredeep. Int J Earth Sci 108:2209–2232

Sant K, Kuiper KF, Rybár S et al (2020) 40Ar/39Ar geochronology using high sensitivity mass spectrometry: examples from middle Miocene horizons of the Central Paratethys. Geol Carpath 71:166–182. https://doi.org/10.31577/GeolCarp.71.2.5

Schubert G, Safoschnik T, Supper R et al (1999) B1 Das Becken von Obermarkersdorf. Arbeitstagung der Geologischen Bundesanstalt 1999—Retz-Hollabrunn. Geologische Bundesanstalt, Wien, pp 279–286

Šegvić B, Mileusnić M, Aljinović D et al (2014) Magmatic provenance and diagenesis of Miocene tuffs from the Dinaride Lake System (the Sinj Basin, Croatia). Eur J Mineral 26:83–101. https://doi.org/10.1127/0935-1221/2013/0025-2350

Šegvić B, Lukács R, Mandic O et al (2023) U–Pb zircon age and mineralogy of the St. Georgen halloysite tuff shed light on the timing of the middle Badenian (mid-Langhian) transgression, ash dispersal and palaeoenvironmental conditions in the southern Vienna Basin, Austria. J Geol Soc. https://doi.org/10.1144/jgs2022-106

Ślączka A (1977) Rozwój osadów miocenu z otworu wiertniczego Sucha IG-1. Kwart Geol 21:405–406 ((**in Polish**))

Slavík J (1956) Zpráva o dacitových tuffitech v mořském tortónu vněkarpatské pánve na Moravě. Věstník Ústředního Ústavu Geologického 31:1 ((**in Czech**))

Sliwinski JT, Guillong M, Liebske C et al (2017) Improved accuracy of LA-ICP-MS U-Pb ages of Cenozoic zircons by alpha dose correction. Chem Geol 472:8–21. https://doi.org/10.1016/j.chemgeo.2017.09.014

Sliwinski JT, Guillong M, Horstwood MSA et al (2022) Quantifying long-term reproducibility of zircon reference materials by U-Pb LA-ICP-MS dating. Geostand Geoanal Res 46:401–409. https://doi.org/10.1111/ggr.12442

Steininger F, Seneš J (eds) (1971) M1 Eggenburgien. Die Eggenburger Schichtengruppe und ihr Stratotypus. Chronostratigraphie und Neostratotypen, Miozän der zentralen Paratethys 2:1–827. VEDA, Bratislava.

Stráník Z, Adámek J, Brzobohatý R et al. (2021) Geologie Vnějších Západních Karpat a jihovýchodního okraje Západoevropské platformy v České republice. Česká geologická služba, Praha. (in Czech)

Szakács A, Zelenka T, Márton E et al (1998) Miocene acidic explosive volcanism in the Bükk Foreland, Hungary: identifying eruptive sequences and searching for source locations. Acta Geol Hung 41:413–435

Tejkal J (1958) Spodnomiocenní (?) písky mezi Šatovem a Chvalovicemi a jejich fauna. Časopis Moravského Muzea v Brně 43:85–94 ((**in Czech**))

Tišnovská V, Kratochvíla L, Maslaňáková J et al. (1998) Jezernice – hydrogeologický průzkum ložiska cihlářské suroviny. Unigeo, pr. Zlaté Hory – ČGS Geofond, Praha. (in Czech)

Tomanová Petrová P, Švábenická L (2007) Lower Badenian biostratigraphy and paleoecology: a case study from the Carpathian Foredeep (Czech Republic). Geol Carpath 58:333–352

Trinajstić N, Brlek M, Gaynor SP et al (2023) Provenance and depositional environment of middle Miocene silicic volcaniclastic deposits from Mt. Medvednica (North Croatian Basin, Carpathian-Pannonian Region). J Volcanol Geotherm Res 443:107917. https://doi.org/10.1016/j.jvolgeores.2023.107917

Turco E, Bambini AM, Foresi L et al (2002) Middle Miocene high-resolution calcareous plankton biostratigraphy at Site 926 (Leg 154, equatorial Atlantic Ocean): palaeoecological and palaeobiogeographical implications. Geobios 35:257–276. https://doi.org/10.1016/S0016-6995(02)00064-5

Turco E, Cascella A, Gennari R et al (2011) Integrated stratigraphy of the La Vedova section (Conero Riviera, Italy) and implications for the Burdigalian/Langhian boundary. Stratigraphy 8:89–110

Wade BS, Pearson PN, Berggren WA et al (2011) Review and revision of Cenozoic tropical planktonic foraminiferal biostratigraphy and calibration to the geomagnetic polarity and astronomical time scale. Earth-Sci Rev 104:111–142. https://doi.org/10.1016/j.earscirev.2010.09.003

Wendt I, Carl C (1991) The statistical distribution of the mean squared weighted deviation. Chem Geol Isot Geosci 86:275–285. https://doi.org/10.1016/0168-9622(91)90010-T

Wiedenbeck M, Allé P, Corfu F, Griffin WL, Meier M, Oberli F et al (1995) Three natural zircon standards for U-Th-Pb, Lu-Hf, trace element and REE analyses. Geostand Newsl 19(1):1–23. https://doi.org/10.1111/j.1751-908X.1995.tb00147.x

Wotzlaw JF, Hüsing SK, Hilgen FJ, Schaltegger U (2014) High-precision zircon U–Pb geochronology of astronomically dated volcanic ash beds from the Mediterranean Miocene. Earth Planet Sci Lett 407:19–34

Zádrapa M (1988) Přítomnost vulkanoklastických sedimentů v souvrství karpatu v oblasti Ždánické elevace. Zemni Plyn a Nafta 33:323–331 ((**in Czech**))

Zapfe H (1956) Die geologische Altersstellung österreichischer Kohlenlagerstätten nach dem gegenwärtigen Stand der Kenntnis. Berg- Huttenmann Monatsh 101:71–81

Zorn I (2015) Mittelmiozäne Ostrakoden aus dem Aflenz-Becken (Ostalpen, Österreich). In: Schuster R, Knoll T (eds) Arbeitstagung 2015 der Geologischen Bundesanstalt. Geologie der Kartenblätter GK50 ÖK 103 Kindberg und ÖK 135 Birkfeld, Mitterdorf im Mürztal 21.–25. September 2015, pp 144–150.

Szabó Zs (2002) Cirkonmorfológiai vizsgálatok a Bükkalja miocén piroklasztit sorozatain. MSc Thesis, Eötvös Loránd University, Budapest, 111 p. (in Hungarian)

Authors and Affiliations

Lukács Réka[1,2,3] · Nehyba Slavomír[4] · Guillong Marcel[5] · Roetzel Reinhard[6] · Iglseder Christoph[6] · Harangi Szabolcs[1,3] · Ćorić Stjepan[6] · Gallhofer Daniela[7] · Petrelli Maurizio[8] · Tomanová Petrová Pavla[9]

✉ Lukács Réka
lukacs.reka@csfk.org

Guillong Marcel
marcel.guillong@eaps.ethz.ch

Roetzel Reinhard
roetzel.reinhard@gmail.com

Iglseder Christoph
Christoph.Iglseder@geosphere.at

Harangi Szabolcs
harangi.szabolcs@ttk.elte.hu

Gallhofer Daniela
daniela.gallhofer@uni-graz.at

Petrelli Maurizio
maurizio.petrelli@unipg.it

Tomanová Petrová Pavla
pavla.petrova@geology.cz

[1] MTA–HUN-REN CSFK Lendület "Momentum" PannonianVolcano Research Group, HUN-REN Research Centre for Astronomy and Earth Sciences, Institute for Geological and Geochemical Research, Budaörsi út 45, Budapest 1112, Hungary

[2] HUN-REN CSFK, MTA Centre of Excellence, Konkoly Thege Miklós út 15-17, Budapest 1121, Hungary

[3] Department of Petrology and Geochemistry, Institute of Geography and Earth Sciences, Eötvös Loránd University, Pázmány Péter sétány 1/C, Budapest 1117, Hungary

[4] Department of Geological Sciences, Faculty of Science, Masaryk University, Kotlářská 2, 611 37 Brno, Czech Republic

[5] ETH Zürich, Earth Sciences Department—Institute of Geochemistry and Petrology, Clausiusstraße 25, 8092 Zurich, Switzerland

[6] GeoSphere Austria, Neulinggasse 38, 1030 Vienna, Austria

[7] Institute of Earth Sciences, NAWI Graz Geocenter, University of Graz, Universitätsplatz 2/II, 8010 Graz, Austria

[8] Department of Physics and Geology, University of Perugia, Piazza Università 1, 06123 Perugia, Italy

[9] Czech Geological Survey, Leitnerova 22, 602 00 Brno, Czech Republic